Delft University of Technology

Master of Science in Life Science and Technology
Master Thesis Project

Estimation of kinetic parameters of the acetogen *Clostridium autoethanogenum* on carbon monoxide

Charilaos Korkontzelos
(5213126)

Project duration
01/09/2021-14/06/2022

Thesis committee
Assoc. dr.ir.R.Kleerebezem
Dr.ir.D.Weissbrodt
Assoc.dr.A.Straathof
Daily supervisor
Maxim Allaart

14/06/2022

Abstract

The increasing demands for chemicals and fuels combined with the fuel versus food competition over first generation feedstocks requires the development of more sustainable alternatives. Syngas fermentation offers a sustainable production of fuels and recycling of gaseous and solid waste utilizing gas fermenting bacteria. Acetogens, such as *Clostridium autoethanogenum* (CA) can grow on syngas (CO, CO_2 and H_2) and produce acetate and ethanol via the Wood-Ljungdahl pathway (WLP). Numerous studies have been conducted to optimize the ethanol production by changing different parameters such as the pH, the mineral medium and the ingas composition. These changes can be effectively predicted through kinetic modelling, which requires the knowledge of key kinetic parameters such as the maximum biomass specific substrate uptake rate and the maximum growth rate. Batch fermentation is not a realistic option considering the low solubility of gases such as CO in the liquid, while obtaining the kinetic parameters in chemostats by increasing the dilution rate can be time intensive. To acquire these parameters, CA was cultivated in chemostats and was grown on carbon monoxide as the sole energy and carbon source. Feeding disturbances were carried out by increasing the CO molar fraction in the inlet gas for a short period of time to ensure constant biomass concentration levels. Continuous off-gas analysis revealed that the fermentation is mass transfer limited until the end of the pulse experiments at 85% of CO in the inlet gas. A biomass specific substrate uptake rate of $89.1 \pm 0.23\ mmol/g_{DCW}/h$ was calculated, which is the highest value achieved so far in literature.The calculated growth rate was $0.083\ h^{-1}$. pH profile provided evidence about the metabolism of the microorganism, while the increase of CO_2 to CO yield at higher CO molar fractions was closely related to acetate reduction to ethanol so that the cells can regulate their metabolism.

Contents

1 Introduction

The growing industrialization of many countries during the last decades as well as the rapid increase in the world population has led to a tremendous increase in chemicals and fuels consumption. Given the current consumption rate, fossil fuels are predicted to run out in this century [1]. Furthermore, first generation feedstocks, which can be efficiently used for producing biofuels, are in direct competition with human consumption [2]. It is therefore important to look for more sustainable and environmentally friendly alternatives. Syngas, a mixture of CO, CO_2 and H_2, is produced as a by-product of the steel mill industries as well as from the gasification of solid fuels, solid waste, and biomass [3]. The conventional method of treating syngas is chemically via the Fisher-Tropsch process to produce bioethanol [4]. Nevertheless, this process is quite energy demanding as it operates at high temperatures and pressures (190-350°C and 20-40 bars) [5]. Moreover, the presence of impurities such as sulfur compounds in the gas mixture, as well as the need for certain H_2 to CO ratio to achieve high yields, make it a non-applicable option [4]. Another option for producing biofuels from syngas is via syngas fermentation. There is a certain type of bacteria, known as acetogens, which can be utilized as biocatalysts to produce acetate, ethanol, and butanediol [6].

Two of the many acetogenic bacteria that have been studied for their syngas fermenting properties are *C.autoethanogenum* (CA) and *C.ljungdahlii* which belong to the *Clostridium* genus. These anaerobic autotrophic bacteria follow the Wood-Ljungadhl pathway (WLP) to primarily produce acetate and ethanol. They have the ability to grow on carbon monoxide which can be utilized as both energy and carbon source. Alternatively, H_2 can be used as the energy source with CO_2 providing the carbon required according to Reactions 1-4 [7].

$$4CO + 2H_2O \rightarrow CH_3COOH + 2CO_2 \tag{1}$$

$$6CO + 3H_2O \rightarrow CH_3CH_2OH + 4CO_2 \tag{2}$$

$$4H_2 + 2CO_2 \rightarrow CH_3COOH + 2H_2O \tag{3}$$

$$6H_2 + 2CO_2 \rightarrow CH_3CH_2OH + 3H_2O \tag{4}$$

This biochemical pathway, also known as reductive acetyl-CoA pathway, consists of two branches, the methyl and carbonyl branch. In the methyl branch, six reductive steps are required in order to get the methyl group of acetyl-CoA starting from CO_2. If only CO is present in the inlet gas, a further step is required which is the oxidation of CO to CO_2 via the monofunctional CO dehydrogenase (CODH). In the carbonyl branch, CO_2 is reduced back to CO, which serves as the carbonyl group of acetyl-CoA, via the bifunctional CODH. The same enzyme also catalyzes the formation of acetyl-CoA along with acetyl-CoA synthase (ACS) [3].
Once acetyl-CoA is formed, ethanol can be produced in two different ways. The first one is through the direct pathway, which consists of reduction of acetyl-CoA to acetaldehyde catalyzed by aldehyde dehydrogenase (Aldh) and then subsequent reduction of acetaldehyde to ethanol via the alcohol dehydrogenase (Adh) enzyme. The second way is by utilizing the indirect pathway which includes reduction of acetyl-CoA to acetate by acetate kinase (ACK) with the gain of one mole of ATP [8]. Acetate is then further reduced to acetaldehyde catalyzed by the aldehyde ferredoxin oxidoreductase (AOR) and final reduction to ethanol. Studies have shown that ethanol is produced only through the indirect pathway [9, 10]. The main reason for that is the loss of one mole of ATP in the methyl-branch for the reduction of formate to 10-formyl-H_4 folate, which can only be compensated through the indirect pathway resulting in no net ATP formation during the pathway [11]. The energy required for the different reactions is provided by electron carriers. Ferredoxin (Fd_{ox})/reduced ferredoxin (Fd^{-2}), $NADPH/NADP^+$ and $NADH/NAD^+$, are the most known in the WLP and can accept and deliver electrons to drive the

different reactions. These electron carriers are balanced by enzyme complexes, which can couple reactions that cannot occur spontaneously with reactions that release energy to regulate their metabolism. The most important complexes are the NADH-dependent reduced ferredoxin:$NADP+$ oxidoreductase (Nfn) which couples the oxidation of one mole of reduced ferredoxin and one mole of NADH with the reduction of 2 moles of NADPH, and the reduced ferredoxin:NAD^+ oxidoreductase (RnfA-G), which couples the oxidation of one mole of reduced ferredoxin with the reduction of one mole NADH to release two moles of protons. In this way, a proton motive force is generated to drive the ATP synthase and make the ATP that the cells require for maintenance and to produce acetate, ethanol and biomass [11] (Figure 1).

Based on this metabolic pathway, a great number of papers have been published on the impact of different parameters such as the pH, the syngas composition, the ingas flow rate and the mineral medium composition on the final product ratio. [12, 13, 4, 14, 15, 16]. The extent of the impact of each of these parameters can be visualized using kinetic models. Kinetic modeling gives a better understanding of the cell mechanism. It is widely used to predict the behavior of a system based on the knowledge that has already been acquired from different studies [17]. However, to optimize the process parameters, knowledge of the kinetics, such as the maximum growth rate and the maximum substrate consumption rate, is important.

A common way of estimating the kinetic parameters of a microorganism is in a batch fermentation. When all growth nutrients are in excess,the microorganism can grow exponentially. During this phase, the microbial growth rate is equal to the maximum. However, gas fermentation is more complex. Carbon monoxide has a very low solubility in water (saturated concentration of CO under 1 atmosphere of pure gas is only 0.983 mmol/L) [18], while the gas-liquid mass transfer rate in lab-scale bioreactors is usually the limiting step [19]. Thus, fermenting a CA culture in batch mode cannot be applied because the soluble substrate concentration is low to allow the cells to reach the exponential growth phase. Fed-batch fermentation using a constant supply of gas has also disadvantages related to mass transfer limitation. On the other hand, cultivating the cells in continuous cultures with a constant supply of gas until reaching steady-state could be the solution to this problem. Continuous cultures under steady state conditions are considered to be well-controlled systems with reliable results [20]. Nevertheless, it can be very time consuming to obtain several steady-states until reaching the maximum growth rate [21]. Studying the effect of disturbances during steady-state conditions can provide significant data regarding the kinetic parameters of the microorganism [21]. The aim of this work was to estimate the kinetic parameters of the acetogen *C.autoethanogenum* using CO as the only energy and carbon source, since only limited papers have been published for CO fermentation [22, 14, 23], which would enable to gain further insight into gas fermentation. The microorganism was grown in chemostat cultures and once steady-state conditions were reached, pulse feeding experiments were conducted by increasing the partial pressure of carbon monoxide in the inlet gas for a short period of time in order to estimate the biomass specific consumption rate at different partial pressures until reaching the maximum. Continuous off-gas analysis gave significant information related to the product spectrum while pH profile gave clues about the metabolism of the microorganism.

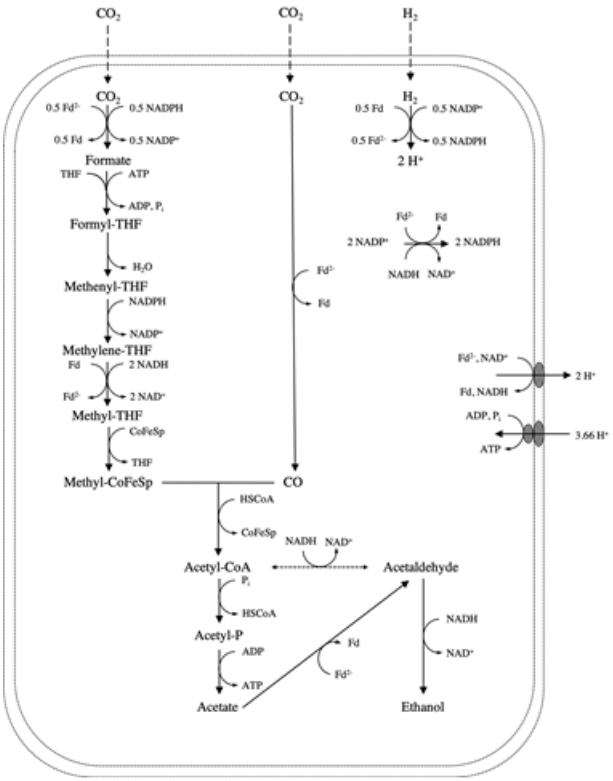

Figure 1: The Wood-Ljungdahl pathway for acetogenic bacteria and reduction of acetyl-CoA to ethanol and acetate. When CO is used as the main electron and carbon source, it is oxidized to CO_2 with one mole of ferredoxin per mole of CO via the monofunctional CODH [24]. One mole of CO_2 is used for the methyl branch and one for the carbonyl branch. In the methyl branch, CO_2 is first reduced to formate with 0.5 moles of NADPH and 0.5 moles of reduced ferredoxin catalyzed by the formate dehydrogenase (Fdh). Next, formate is reduced to 10-formyl-H_4folate catalyzed by 10-formyl-H_4folate synthetase at the expense of one mole ATP [25]. The latter intermediate is converted to 5,10-methelyn-H_4folate which is then reduced to 5,10-methylene-H_4folate with NADPH by methylene-H_4folate dehydrogenase. The final step of the methyl branch includes the reduction to 5-methyl-H_4 folate by methylene-H_4 folate reductase with 2 moles of NADH as reductant and 1 mole of ferredoxin as oxidant [8]. In the carbonyl branch, CO_2 is reduced back to CO by the bifunctional CODH and acetyl-CoA synthase using one mole of reduced ferredoxin. When acetyl-CoA is formed, it is reduced to acetate via the acetate kinase with the gain of one mole of ATP [8]. In the indirect pathway of ethanol formation, acetate is reduced to acetaldehyde via the aldehyde ferredoxin oxidoreductase (AOR) with one mole of reduced ferredoxin. Acetaldehyde is further reduced to ethanol via the alcohol dehydrogenase (Adh) with one mole of NADH. The direct pathway consists of reduction of acetyl-CoA to acetaldehyde and then to ethanol with two moles of NADH in total. The electron carriers are balanced by enzyme complexes such as the Nfn and Rnf complex. The Rnf complex creates a proton motive force for ATP generation [11].

2 Materials and Methods

2.1 Cultivation of *Clostridium autoethanogenum*

2.1.1 Microbial strain

A culture of the Clostridium autoethanogenum DSM strain 10061 was acquired from colleagues at Wageningen University (WUR) in batch bottles at an exponential growth phase.

2.1.2 Composition of medium with yeast extract

For batch bottle and bioreactor cultivation during fed batch, medium proposed by Diender et al. [26] was used, containing per liter the following: 0.9 g NH_4Cl, 0.9 g NaCl, 0.2 g $MgSO_4$ x $7H_2O$, 0.75 g KH_2PO_4, 1.5 g K_2HPO_4, 0.02 g $Cacl_2$ x $2H_2O$, 0.5 mg Na-resazurin, 1 mL of acid trace elements and 0.2 mL of base trace elements.The alkaline stock solution concentrated 5000x contained per liter: 400 mg NaOH, 17.29 mg Na_2SeO_3 , 1033 mg Na_2WO_4 x $2H_2O$ and 24.2 mg Na_2MoO_4 x $2H_2O$. The acidic trace elements solution concentrated 1000x contained per liter: 10 mL HCl 25%, 1.50 g $FeCl_2$ x $4H_2O$, 2.50 g $FeCl_3$ x $6H_2O$, 70 mg $ZnCl_2$, 100 mg $MgCl_2$ x $4H_2O$, 6 mg H_3BO_3, 190 mg $CoCl_2$ x $6H_2O$, 2 mg $CuCl_2$ x $2H_2O$, 24 mg $NiCl_2$ x $6H_2O$ and 36 mg Na_2MoO_4 x $2H_2O$. After sterilizing the medium at 121°C, it was stirred and sparged with N_2 for at least 24 hours in order to strip out the oxygen. Next, 20 mL/L of yeast extract stock solution (25 g/L), 2 mL/L filter-sterilized vitamin solution and 0.75 g/L of sterile L-cysteine-HCl x H_2O were added. The vitamin stock was concentrated 1000x and contained the following per liter: 20 mg biotin, 200 mg nicotinamide, 1000 mg p-aminobenzoic acid, 200 mg thiamin, 1000 mg pantothenic acid (vitamin B5), 500 mg pyridoxamine, 100 mg cyanocobalamine, and 100 mg riboflavine.

2.1.3 Chemically defined medium without yeast extract

In order to be able to accurately calculate the carbon and electron balances during steady state conditions and compare the results with more recent publications, a chemically defined medium without yeast extract (YE) was used as described by Valgepea et al. [15]. The mineral medium contained per liter: 0.5 g $MgSO_4$ x $6H_2O$, 0.2 g NaCl , 0.1 g $CaCl_2$, 2.65 g NaH_2PO_4 x $2H_2O$, 0.5 g KCl , 2.5 g NH_4Cl , 0.017 g $FeCl_3$ x $6H_2O$, 0.5 mg Na-resazurin, 10 ml trace metal solution (TMS).The TMS contained per liter: 1.5 g trisodium nitrilotriacetate, 3 g $MgSO_4$ x $7H_2O$, 0.5 g $MnSO_4$ x H_2O , 1 g NaCl , 0.667 g $FeSO_4$ x $7H_2O$, 0.2 g $CoCl_2$ x $6H_2O$, 0.2 g $ZnSO_4$ x $7H_2O$, 0.02 g $CuCl_2$ x $2H_2O$, 0.014 g $Al_2(SO_4)_3$ x $18H_2O$, 0.3 g H_3BO_3 , 0.03 g $NaMoO_4$ x $2H_2O$, 0.02 g Na_2SeO_3 , 0.02 g $NiCl_2$ x $6H_2O$ and 0.02 g Na_2WO_4 x $2H_2O$. After sterilizing the medium at 121°C, it was stirred and sparged with N_2 for at least 24 hours in order to strip out the oxygen. Next, 0.5 g/L of sterile L-cysteine-HCl x H_2O and 2 mL/L concentrated filter-sterilized vitamin solution were added. The B-vitamin solution contained per liter: 100 mg Biotin , 100 mg Folic acid , 50 mg Pyridoxine Hydrochloride , 250 mg Thiamine-HCl x H_2O , 250 mg Riboflavin , 250 mg Nicotinic acid , 250 mg Calcium pantothenate , 250 mg Vitamin B12 , 250 mg 4-Aminobenzoic acid and 250 mg Thioctic acid.Moreover, 10 mL of 37% HCl was added to ensure the sterility of the medium. The medium was ready to be used only when it became completely transparent indicating that the cysteine was completely reduced and no oxygen was present.

2.1.4 Preparation of precultures

In order to cultivate *C.autoethanogenum* cells in a 3L bioreactor, precultures were prepared in 120 mL batch bottles with 50 mL working volume. The headspace before the autoclave was exchanged for N_2 in order to strip out the oxygen.After sterilizing the medium and adding the sterile components, the headspace was exchanged for 100% CO. After that, the bottles were inoculated with 1 mL of actively growing CA culture. Depending on the optical density and pH of the inoculum, lag phase could last for

3-5 days after which the culture would reach the exponential phase and could be used for inoculation or further cell propagation.

2.1.5 Bioreactor operation

For fed-batch fermentation, a glass jacketed 3L bioreactor was used. 2 different working volumes of 2 L and 1.6 L were tested. The reason for lowering the working volume is explained in Section 2.2. L-cysteine-HCl x H_2O and vitamins were added after sterilisation and sparging the reactor with N_2 for at least 24 hours to ensure anaerobic conditions. When L-cysteine was completely reduced and pH was set to 5.5, the reactor was inoculated with 100 and 150 mL of actively growing preculture for the first and third fed-batch experiment respectively. During fermentation, temperature was maintained at 37°C using a thermostat bath (E300, Lauda, Germany). To prevent culture broth evaporation, the off-gas was cooled at 5°C using a cryostat. pH was measured with a pH probe connected to an Applicon controller connected to a MFCS software.

A specific startup procedure was used to prevent toxification of the microorganism at low biomass concentrations after inoculation. The protocol can be found in Appendix A.2.
The reactor was continuously agitated and fed with gas. The conditions for the first and third fed-batch cultures were initially the same until switching to chemostat at an optical density at 660 nm (OD_{660}) of 0.6-0.7.
The first and second chemostat were operated at an agitation speed of 500 rpm, a gas flow rate of 100 ml/min with 20% CO and 80% N_2 and a dilution rate of $0.008^{-}h$. The last chemostat was operated at the same flow rate of 100 ml/min but at lower CO molar fraction in the gas (10% CO , 90% N_2) in order to have a bigger range of partial pressures for the CO pulse experiments. The agitation speed was 600 rpm. A dilution rate of $0.01^{-}h$ was achieved. Table 1 summarizes the operating conditions for the three chemostat operations.

Table 1: Operating conditions for the three chemostat operations.

Parameters	SS1	SS2	SS3
Gas composition	20% CO , 80% N_2	20% CO , 80% N_2	10% CO , 90% N_2
Agitation speed (rpm)	500	500	600
Dilution rate (1/h)	0.008	0.008	0.01
Working volume (L)	2.0	2.0	1.6
YE in feed medium	YES	NO	NO
Gas flow rate (ml/min)	100	100	100
pH	5.5	5.5	5.5

2.2 kla experiments

As mentioned in Chapter 1, gas-liquid mass transfer is one of the main bottlenecks of syngas fermentation. The solubility of CO in the liquid is very low [19] which prevents the optimal growth of the culture since the amount of the substrate that the reactor can supply is lower than the one the cells need to grow. A feasible way of increasing the mass transfer rate is by increasing the agitation speed which will subsequently increase the volumetric mass transfer coefficient kla [19]. It is therefore possible to estimate the maximum substrate uptake rate by increasing the stirring speed until the fermentation is no longer mass transfer but kinetically limited. Taking that into account, a kla experiment was conducted as proposed by Garcia et al. [27] using *C.autoethanogenum* broth. Briefly, this dynamic method is based on measuring the concentration of dissolved oxygen in the medium by absorption or disorption of it. Initially oxygen is stripped out from the reactor by sparging with N_2 until dissolved oxygen is zero. Then air is supplied again, until reaching the oxygen saturation concentration in the medium. Nitrogen bubbling continues until oxygen concentration is zero. Finally, air is supplied again

in the reactor and the increase in oxygen concentration is measured with time. After determining the volumetric mass transfer coefficient in oxygen, the respective parameter can be estimated for carbon monoxide by using the diffusion coefficients of the two gases ($2.03 * 10^{-5}$ cm^2/s for CO and $2.0 * 10^{-5}$ cm^2/s for air [28]).

This procedure was performed in duplicates for 5 different stirring speeds (300,500,600,700 and 800 rpm) in a 3L bioreactor at 37°C and a gas flow rate of 100 ml/min. The working volume was 2 L. During the 800 rpm test, there was a leakage in the reactor due to extensive foaming. Therefore, it was decided to decrease the working volume for the next fed-batch experiment from 2 L to 1.6 L. Futhermore, another complication of these experiments was the calibration of the dissolved oxygen (DO) probe. Calibrating the probe in the cell broth resulted in different oxygen saturation coefficients for the different stirring speeds. This could be explained by the fact that the cells were gradually dissolved in the liquid, obtaining a fully transparent medium at the end. As a consequence, the viscosity of the medium was possible altered which could have an impact on the mass transfer rate and therefore the kla values [29]. The graph and the table with the respective kla values for carbon monoxide are given in Appendix B.1.

2.3 Pulse experiments

Since no clear linear trend between the mass transfer coefficient and the agitation speed could be distinguished, it was decided to increase the mass transfer capacity by increasing the driving force for substrate transfer. This can be done by changing the maximum solubility of CO in the liquid by increasing the molar fraction of CO in the inlet gas. Different timespans of 30 minutes and 1 hour were carried out to determine the optimum pulse length until 30% of CO in the inlet gas. For each CO molar fraction, the pulse experiments were performed in triplicates or quadruplicates.Finally, off-gas was diluted with 100 ml/min of N_2 after exceeding 60% of CO in the incoming gas due to the CO detection range of the off-gas analyzer which is between 0 and 40%.

2.4 Off-line analysis

2.4.1 TSS/VSS measurements

To estimate the biomass concentration in dry cell weight per liter, a correlation coefficient between the optical density at 660 nm and g_{DCW}/L was determined according to the protocol given in Appendix A.1. A correlation coefficient (K) of 0.2935 (BC = OD_{660} x K) with an R^2 of 0.998 was measured (Figure A.1).

2.4.2 Analysis of Organic acids and Alcohols

After measuring the OD_{660} of the culture at a certain time point, 2 ml of fermentation sample were filtered using a 0.22 µm membrane filter. High performance liquid chromatography (HPLC) was used to detect ethanol and acetate. Each HPLC sample was run for 30 minutes. The HPLC (Thermo,Germany) was equipped with an Animex HPX-87H column (Biorad) at 60°C linked to an ultraviolet (UV) and refraction index (RI) detector (Thermo,Germany). 1.5 mM phosphoric acid (H_3PO_4) was used as eluent at a flowrate of 0.75 ml/min and 10 µl injection volume. Acetate was determined on the UV/VIS spectrum while ethanol was detected on the RI spectrum. The retention time for ethanol and acetate was 17.5 and 12 minutes respectively.

2.5 On-line analysis

2.5.1 Bioreactor off-gas analysis

Bioreactor continuous off-gas analysis was performed by an X-stream enhanced series process gas analyzer (Emerson,Netherlands). Biomass specific rates ($mmol/g_{DCW}/h$) were calculated by taking

into account the exact composition of the inlet gas, bioreactor liquid working volume (V_L), feeding gas flow rate (Fg_{in}), off-gas flow rate (Fg_{out}) based on the fractional difference of the inert gas N_2 in the feeding and off-gas composition, the molar volume (V_m) of ideal gas (22.4 ml/mmol at 0°C) and the biomass concentration at steady-state (C_x).

2.6 Data analysis

2.6.1 Biomass specific uptake and production rates

Biomass specific uptake (CO) and production rates (CO_2, ethanol, acetate and H_2) during steady state conditions were calculated based on Equations 6 - 10. For the gaseous compounds (CO, CO_2 and H_2), the continuous off-gas analysis was used in order to calculate the consumption or production rates in ml/min. Next, this value was converted to mmol/min using the molar volume at 0°C, because the mass flow controllers are calibrated at STP conditions. Finally, the biomass concentration at each time point and the working volume were used in order to calculate the biomass specific rates in mmmol/gDCW/h. For the liquid compounds, such as ethanol and acetate, the biomass specific rates were determined based on the mass balances for a chemostat as shown below:

$$\frac{dC}{dt} = D * (C_{in} - C_{out}) + q * C_x \tag{5}$$

where, D is the dilution rate (1/h). During steady state, the liquid concentration remains constant thus the left part of Equation 5 equals zero. Furthermore, no acetate or ethanol exists in the mineral medium, so the inflow concentration is also zero resulting in Equations 9 and 10 for ethanol and acetate respectively.

$$q_{CO} = \frac{F_g^{in} * y_{CO\,in} - F_g^{out} * y_{CO\,out}}{C_x * V_L * V_m} \tag{6}$$

$$q_{CO_2} = \frac{F_g^{out} * y_{CO_2\,out}}{C_x * V_L * V_m} \tag{7}$$

$$q_{H_2} = \frac{F_g^{out} * y_{H_2\,out}}{C_x * V_L * V_m} \tag{8}$$

$$q_{ethanol} = \frac{D * C_{ethanol}}{C_x} \tag{9}$$

$$q_{acetate} = \frac{D * C_{acetate}}{C_x} \tag{10}$$

2.6.2 Carbon and electron recovery

Carbon and electron recoveries were defined using the number of carbon atoms, the degree of reduction and the biomass specific rates of the different compounds. The chemical formula used for biomass is $CH_{1.8}O_{0.5}N_{0.2}$ which gives a degree of reduction of 4.2. The relations that were used to calculate them are described below:

$$C\%_{recovery} = \frac{2 * q_{ethanol} + 2 * q_{acetate} + q_{CO_2} + \mu}{q_{CO}} \tag{11}$$

$$e^-\%_{recovery} = \frac{12 * q_{ethanol} + 8 * q_{acetate} + 2 * q_{H_2} + 4.2 * \mu}{2 * q_{CO}} \tag{12}$$

2.6.3 Estimation of mass transfer coefficient kla

The mass transfer coefficient kla (1/h) was estimated for steady state conditions using the mass balance for carbon monoxide in the liquid phase as follows:

$$\frac{dC}{dt} = D * (C_{in} - C_{out}) + kla * (C^* - C_{out}) - q_s * C_x \tag{13}$$

where C^* is the liquid phase concentration in equilibrium with gas (mol/L) and it can be calculated according to Henry's law:

$$C^* = y * p * H \tag{14}$$

where, y is the molar fraction in the gas mixture, p is the total pressure and H is the Henry's constant ($9.83 * 10^{-4}$ mol/L/atm for CO [18]).

The concentration of the compound remains constant during steady-state, so the left part of Equation 13 is zero. Furthermore, taking into account that the solubility of CO in liquid is low, mass transfer is probably the limiting step. This leads to a CO limited system and thus a low residual concentration in the liquid which can be assumed to be close to zero. Finally, no CO is fed through the medium, so the concentration in the inlet is also zero. Thus, the mass balance can be rewritten as follows:

$$kla * C^* = q_s * C_x \rightarrow kla = \frac{q_s * C_x}{C^*} \tag{15}$$

2.7 Theoretical analysis and estimation of kinetic parameters using the thermodynamic approach

To have a rough estimation about the experimental biomass specific uptake rate range, the kinetic parameters can be thermodynamically estimated. To estimate these parameters, it is important to derive the number of electrons transferred per mole of electron donor (CO) in the WLP for both acetate and ethanol formation. In a fermentation process, the electron donor and electron acceptor is the same, so the extraction of the number of electrons transferred requires a further knowledge of the biochemistry of the microorganism. Ethanol and acetate are the main products in the fermentation. For ethanol production, only the indirect pathway is considered based on the information provided in Chapter 1. Figures 2 and 3 show the electron carriers used at each step of the WLP pathway. The redox reactions of Fd_{ox} to Fd^{2-}, NAD^+ to NADH and $NADP^+$ to NADPH involve 2 electrons transferred each. For instance, the reduction of CO_2 to formate involves the oxidation of 0.5 moles of NADPH and 0.5 moles of reduced ferredoxin. Thus, 2 electrons are transferred in total in this step. More electrons are transferred per mole of ethanol because there are more reactions that take place. NADH and NADPH are consumed inside the pathway. NADPH balance is restored via the Nfn complex in which it is produced while NADH is balanced via the Rnf complex which also creates the proton motive force to generate ATP via the ATP synthase. A ratio of 3.66 mol of H^+ per mol of ATP is considered [30].

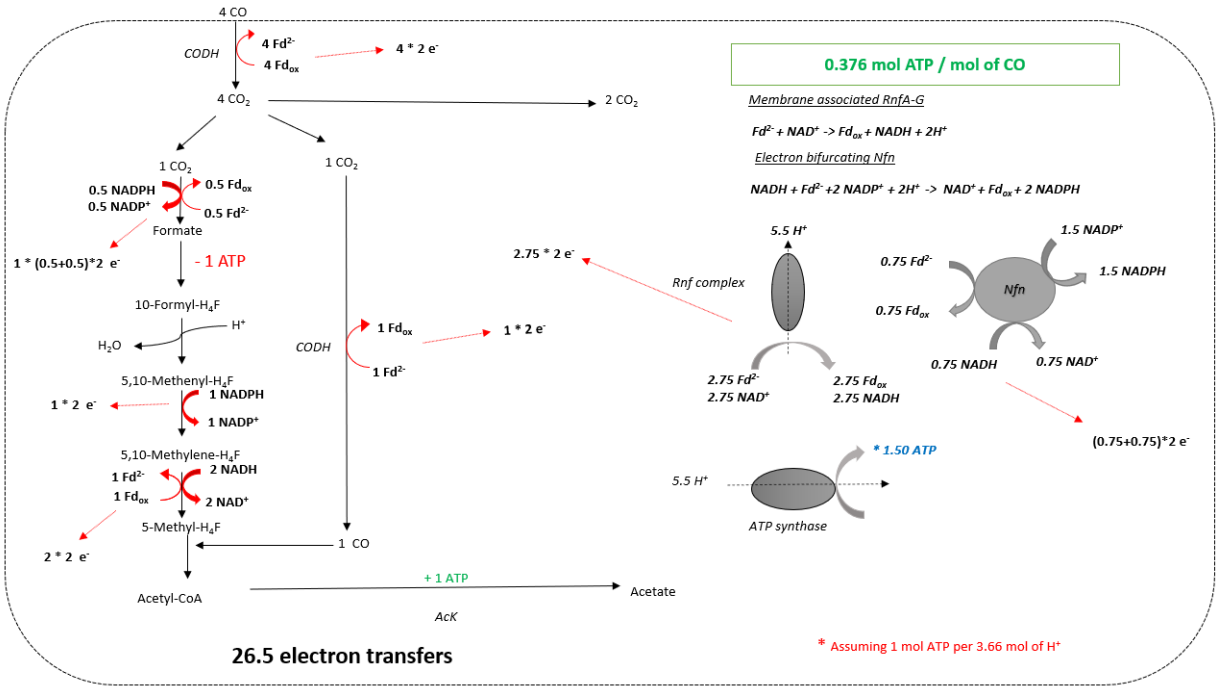

Figure 2: Metabolic pathway for acetate production from CO according to Reaction 1. In the pathway, 5 moles of reduced ferredoxin are produced and 1.5 moles are oxidized to ferredoxin. Furthermore, 1.5 moles of NADPH and 2 moles of NADH are consumed. Of the remaining 3.5 moles of Fd^{2-}, 0.75 moles are used in the Nfn complex to make 1.5 moles of NADPH while 0.75 moles of NADH are also oxidized. This leaves 2.75 moles of Fd^{2-} which are oxidized in the Rnf complex to produce 2.75 moles NADH closing in that way the metabolites balance. 5.5 moles of protons are generated to produce 1.50 moles of ATP per mole of acetate. The electrons transfers of the reactions are given in red arrows leading to a total number of 26.5 per mole of acetate.

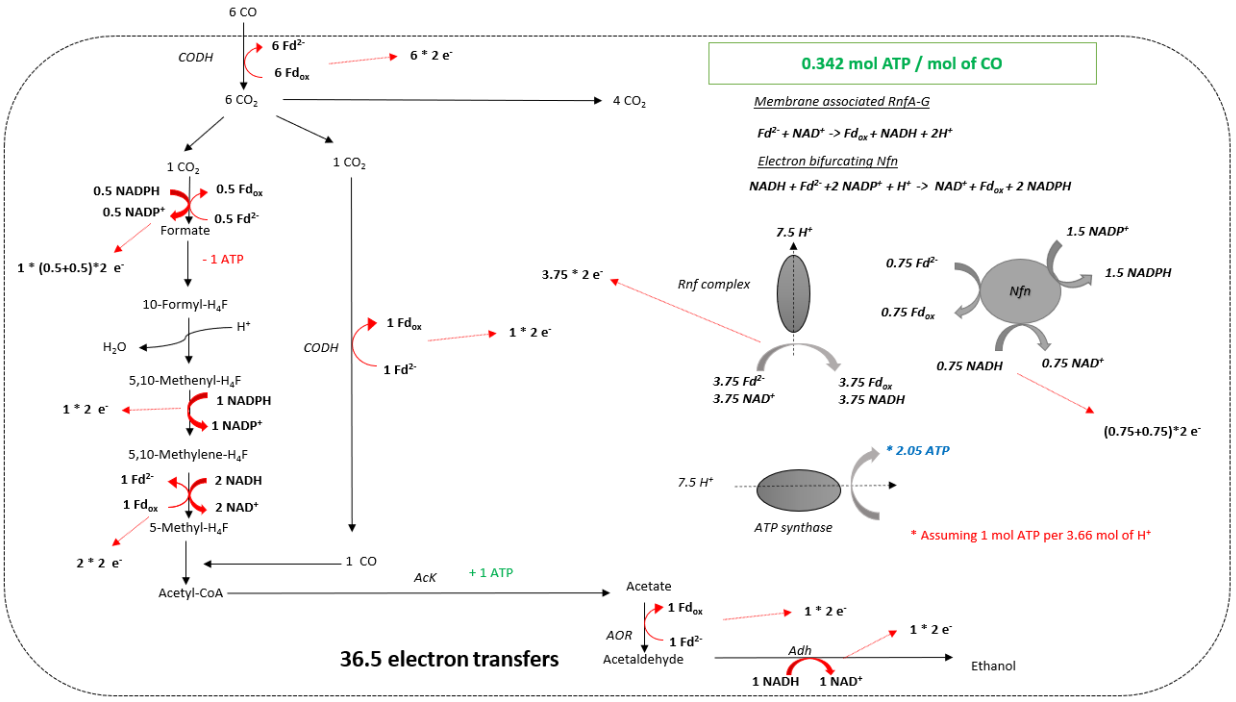

Figure 3: Metabolic pathway for ethanol production from CO according to Reaction 2. In the pathway, 7 moles of reduced ferredoxin are produced and 2.5 moles are oxidized to ferredoxin.Furthermore, 1.5 moles of NADPH and 3 moles of NADH are consumed. Of the remaining 4.5 moles of Fd^{-2}, 0.75 moles are used in the Nfn complex to make 1.5 moles of NADPH while 0.75 moles of NADH are also reduced. This leaves 3.75 moles of Fd^{2-} which are oxidized in the Rnf complex to produce 3.75 moles NADH closing in that way the metabolites balance. 7.5 moles of protons are generated to produce 2.05 moles of ATP per mole of ethanol. The electrons transfers of the reactions are given in red arrows leading to a total number of 36.5 per mole of ethanol.

This electron transfer mechanism results to 26.5 and 36.5 electron transfers to form one mole of acetate and ethanol respectively. The number of electron transfers is defined per mole of electron donor. 4 moles of CO are required to produce one mole of acetate and 6 moles to form one mole of ethanol. Thus, the number of electron transferred is 6.625 per mole of CO for acetate formation and 6.08 per mole of CO for ethanol. Once this number has been estimated, the kinetic parameters can be determined. The calculations and equations that were used, they can be found in Appendix C.1. To derive these numbers, some assumptions were made. The most important ones are the formula used for calculating the Gibbs energy dissipation as proposed by Heijnen and Van Dijken [31], the maximum electron transfer capacity in catabolism (-3mol_e^- /mol_x/h) also proposed by Heijnen et al. [32] and the Gibbs energy for maintenance [33]. Among these assumptions, the maximum electron capacity is mostly used when an external electron acceptor is present. In this case, there is no terminal electron acceptor since CO is used as both electron donor and acceptor, however the number can be used to obtain a rough estimation of the kinetic parameters. The anabolic, catabolic and metabolic reactions for acetate and ethanol formation were derived by using the Gibbs energy change of formation, and the λ_{cat}, which is the number of times that catabolism has to run to produce one Cmole of biomass, was determined for both products (16.13 for acetate and 17.75 for ethanol).Next, the maximum biomass yield for acetate and ethanol were estimated and found equal to 1.35 g_{DCW}/mol_{CO} and 1.24 g_{DCW}/mol_{CO} respectively. Eventually, the maximum substrate uptake rate for acetate and ethanol was estimated to be 60.0 and 65.0 $mmol_{CO}/g_{DCW}/h$ for acetate and ethanol respectively while a maximum growth rate of 0.064 and 0.063 h^{-1} for acetate and ethanol were derived.

2.8 Biomass yield estimation using the ATP balancing method

The maximum biomass yield can also be estimated using the ATP produced in catabolism and consumed in anabolism. Figures 2 and 3 show that 0.376 and 0.342 moles of ATP are produced per mol of CO for acetate and ethanol production respectively. In anabolism , ATP is consumed to produce biomass. Due to the fact that an ATP requirement for anabolism, when CO is used as carbon source, could not be found, the theoretical yield for CO_2 (-3.73 moles of ATP per Cmol biomass) is used [34]. Considering that the cells can also grow on CO_2 as a carbon source it is assumed that the ATP requirements for anabolism are similar. Next, taking into account that the ATP produced has to be equal to the ATP consumed, the λ_{cat} was derived (9.92 for acetate and 10.91 for ethanol) using Equation C.21 resulting in a maximum biomass yield of 2.05 and 1.89 g_{DCW}/mol_{CO} for acetate and ethanol respectively. Further information are given in Appendix C.2.

3 Results

3.1 Chemostat culture experiments overview

Three different steady states were achieved using CO as the only energy and carbon source. The first chemostat culture was grown using the yeast extract containing feed medium to ensure optimal microbial growth. Steady state was reached after 405 hours of fermentation. After characterising it, the feed medium was switched to the chemically defined one in order to be able to determine the carbon and electron balances more accurately. Before reaching steady-state, the fermentation was stopped due to a CO leakage (1520 hours of operation), so no data are available. For the second chemostat that reached steady-state after 830 hours of fermentation, the working volume was decreased to 1.6 L as mentioned in Section 2.2. Finally, to compare the effect of the absence of yeast extract on the concentration of biomass and products, a third and final chemostat was started under the same operating conditions as the first chemostat using the chemically defined medium. To reach steady state as soon as possible, the effluent of the reactor that the pulse experiments were carried out, was used as the influent of this reactor. The steady state for this chemostat was achieved after 660 hours. Figure 4 illustrates the data acquired from the three different steady states. The system was considered to be in steady state when the biomass concentration was ±10% than the average concentration. Biomass yield was derived by dividing the growth rate (h^{-1}) by the biomass specific uptake rate of carbon monoxide ($mmol/gDCW/h$) and then multiplying by 1000 to get the units in g_{DCW}/mol_{CO}.

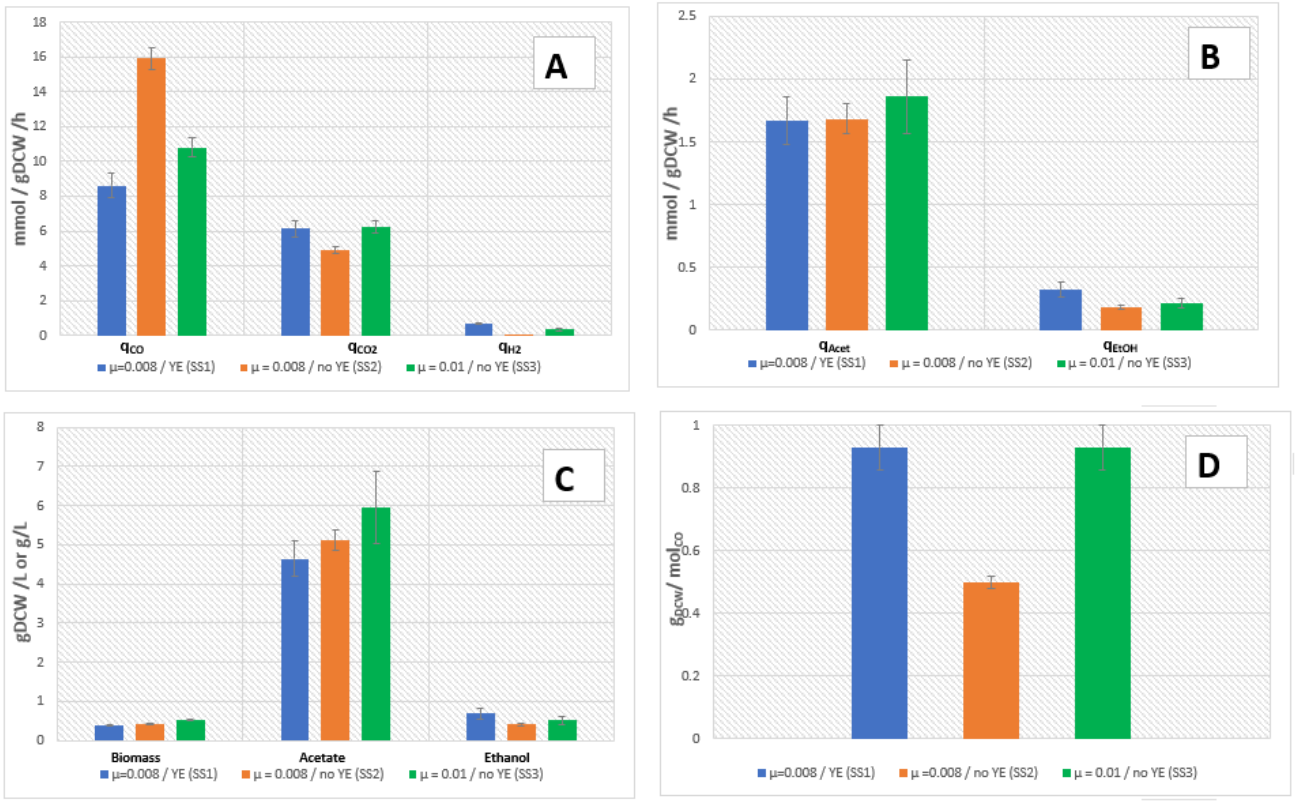

Figure 4: Specific growth rate-dependent growth characteristics in CO *C.autoethanogenum* chemostats grown on mineral medium with or without yeast extract. (A) Specific gas uptake and production rates. (B) Specific by-product production rates. (C) Biomass and by-product concentrations. (D) Biomass yield. Growth rate is given in h^{-1}.The operating conditions for each chemostat can be found in Table 1.

Comparing steady-states 1 and 2 which differ only in the presence of yeast extract in the feed mineral medium, it is seen that the biomass concentration levels are very similar (0.39 ±0.01 for SS1 vs 0.41±0.02 for SS2) with low standard deviations between the samples at different time points. On the other hand, the biomass specific uptake rate is almost 100% higher for steady-state 2 (SS2), while the CO_2 biomass specific rate is lower. The higher consumption rate at the same dilution rate can also explain the lower biomass yield for SS2.

Carbon dioxide is produced in both catabolic reactions taking place as shown in Reactions 1 and 2. More substrate consumed would result in a higher production rate of CO_2 which it is not seen for SS2. Regarding the fermentation products, acetate and ethanol, the formation of the latter is higher when yeast extract is present, with the average concentration being more than 35% higher. On the other hand, acetate levels are very comparable between the two chemostats (4.65 ±0.46 g/L for SS1 and 5.12 ±0.25 g/L for SS2), since the two steady state concentrations differ only by 9%. Finally, trace amounts of H_2 are produced in SS1 with the partial pressure in the off-gas being 0.002 atm (0.2% of the gas mixture) resulting in a production rate of 0.66 ± 0.05 $mmol/gDCW/h$. No hydrogen production was detected in SS2. So far, H_2 formation has not been reported in literature for CA fermentation using only CO as both carbon and electron source [23, 22]. Therefore, the fact that the cells release small amounts of hydrogen can provide important information about the cell mechanism and further elaboration is required.

Regarding the third and final steady state (SS3), it is observed that the biomass concentration is almost 35% higher than the other two steady states. Furthermore, the substrate uptake rate is also higher compared to SS1, which is related to the mass transfer capacity increase due to the higher agitation speed and lower working volume. Using the values from Table B.2 as well as Equation 15, a kla mass transfer coefficient of 17.1 and 58.2 h^{-1} for SS1 and SS3 respectively is derived. Even though, the kla is more than 3 times higher for SS3, the same increase is not depicted in the biomass specific uptake rate which is higher by 25%. As far as the product spectrum is concerned, acetate concentration is almost 30% and 15% higher compared to SS1 and SS2 respectively while the concentration of ethanol is lower than SS1. The standard deviation for the product concentrations at steady-state is significant (5.95 ±0.93 g/L and 0.51 ± 0.09 g/L for acetate and ethanol respectively), which it can be attributed to the pulse experiments. The constant perturbations from the standard conditions led to a wider range of product concentrations, especially after the one-hour pulses at 40% of CO. Until then, the average acetate and ethanol concentrations were 6.0 ± 0.34 and 0.50 ± 0.05 respectively. Finally, hydrogen gas is also produced with the partial pressure being 0.001 atm and the production rate equal to 0.35 ± 0.08 $mmol/gDCW/h$ which is lower compared to SS1.The same biomass yield is achieved for the first and last chemostat operations (0.93 g_{DCW}/mol_{CO}).

The biomass specific rates were used in order to calculate the carbon and electron balances for the three steady states as shown in Section 2.6.2. Carbon atoms were distributed in time towards ethanol, acetate, carbon dioxide and biomass, while the electrons were allocated towards ethanol, acetate, biomass and H_2. Here, carbon recoveries of 121% ± 3.1% , 56% ± 1.3% and 100% ± 5.9% for the three steady states respectively were achieved. Electron recoveries were 115% ± 5.4%, 52.8% ± 2.5% and 95% ± 12.4%. The higher than 100% carbon and electron recoveries for SS1 can be justified by the presence of yeast extract in the mineral medium which cannot be measured in the HPLC.

For the second steady state, the carbon and electron gap is almost 50%. This could be due to wrong measurements from the continuous off-gas analyzer which it can also be explained by the fact that biomass specific uptake rate is higher and CO_2 specific production rate is lower than the other two steady states. Furthermore, it is notable that hydrogen is produced in both SS1 and SS3 but not in SS2. Since the q-rates cannot be used to extract the carbon and electron recoveries, the closest way to compare the two steady-states is by using the same off-gas values obtained from the first steady-state

in order to see if the carbon and electron gap is improved. In this case, a carbon and electron recovery of 121.9% ± 2.4% and 114.3% ± 5.0% are determined, which are closer to the recoveries derived for the other two steady states.Therefore, the data obtained for SS2 can only be used to compare the biomass and products concentration with SS1 but not the biomass specific gas uptake and production rates due to the aberrations in the off-gas analysis. The carbon and electron balances at different time points for the three steady states can be found in Appendix B.3.

3.2 CO pulse experiments

Since carbon monoxide's solubility in liquid is low, the fermentation operates under a mass transfer limited regime. When steady state has been reached, by increasing the CO % in the inlet gas for a short period of time, the maximum solubility of CO in the liquid increases and so does the mass transfer rate. [35], while the biomass concentration remains at steady state. The short period pulses enable the cells to consume more substrate without increasing their concentration resulting in a higher specific uptake rate. Assuming that the fermentation continues to operate under mass transfer limitation, the rise in the biomass specific uptake rate should remain linear. When the system switches from mass transfer to kinetic limitation, the uptake rate will not follow this linear trend either because the maximum uptake rate or CO toxicity will be reached.

Initially, the pulses were conducted for a period of 30 minutes in order to ensure that the substrate does not inhibit the biomass growth and that the results obtained from the off-gas analyzer are consistent and reliable. Four CO molar fractions were tested starting from 15% until 30% with a step of 5%. After obtaining the results from the continuous off-gas analysis, it was observed that the curve was very steep. Considering that the volume of the headspace (1.4 L) is a bit lower than the liquid working volume (1.6 L), the response time of the system causes a delay in the actual biological observation. This may have indicated that the CO values reached at the end of the pulse were not equal to the CO value that it could have been reached if the pulse was longer. This could lead to an overestimation of the substrate uptake rate, since the substrate consumption would be higher than the real one. For this reason, the pulses were repeated but this time for an hour. According to Figure 5 , it can be seen that the outcome from the 1 hour pulses is more accurate since CO in off-gas reaches stable values, which shows that a constant biomass specific uptake rate has been achieved.

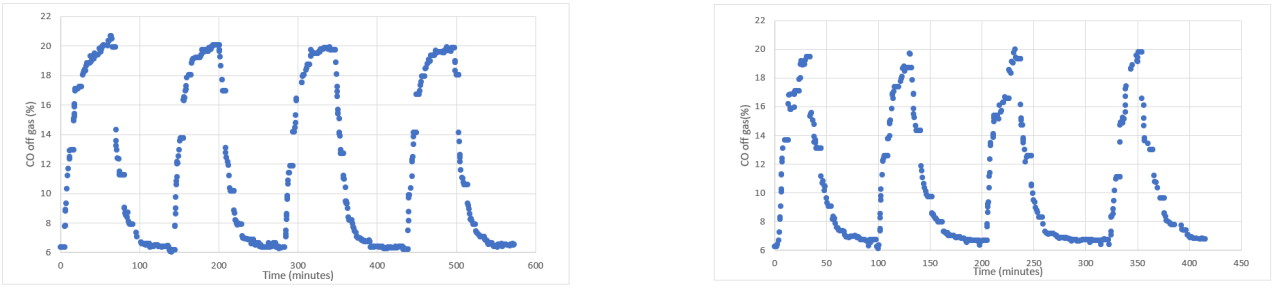

(a) 1 hour pulse

(b) 30 minutes pulse

Figure 5: CO off-gas profile during pulse experiments at 30% CO for (a) 1-hour and (b) 30-minutes pulse

The substrate uptake rate was calculated for every time point using the value of biomass concentration during steady-state (0.53 ± 0.02 gDCW/L). To estimate the substrate uptake rate achieved at every partial pressure as accurately as possible, the values in the horizontal part of the off-gas curve were used and the final rate was derived from the average value. The same procedure was followed for CO_2 and H_2 as well. Figure 6 shows the difference in the biomass specific uptake rate between the 30 minute and 1 hour pulses.

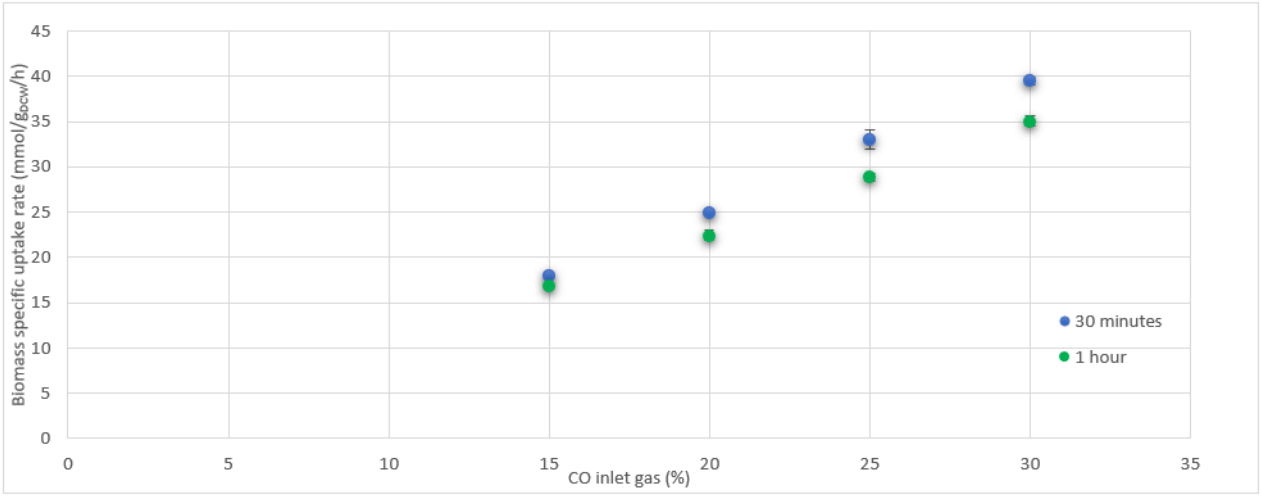

Figure 6: Biomass specific uptake rate (mmol/gDCW/h) for different CO partial pressures at 30 minute (blue) and 1 hour (green) pulses

It is seen that in every CO molar fraction, the biomass specific uptake rate is higher when the pulse is conducted for 30 minutes. Moreover, at 25% and 30% of CO, the q-rate at the 30-minute pulses is more than 10% higher compared to the q-rate achieved for the 1-hour pulses. For this reason, the 30-minute pulses were stopped and only one-hour pulses were conducted for 35% CO and higher. The reason why longer pulses were not tested was to avoid substrate inhibition at higher CO molar fractions and loss of the steady state.

Figure 7 displays the increase of carbon monoxide in the off-gas as measured using continuous off-gas analysis for different CO percentages in the inlet gas. It can be observed that the maximum CO values reached at each molar fraction follow a linear trend with the CO partial pressure in the inlet gas.

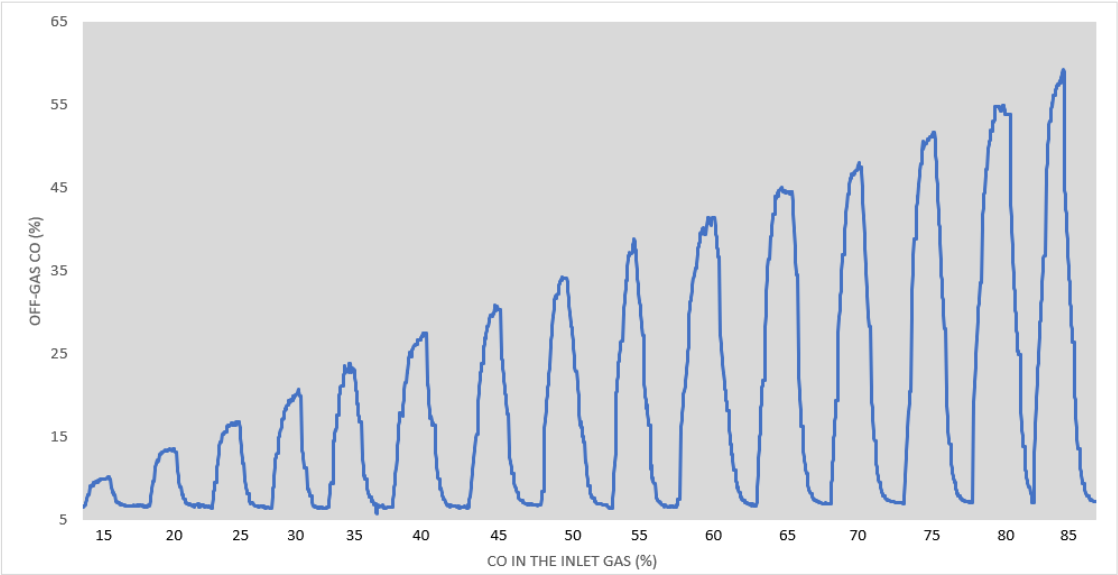

Figure 7: Off-gas results obtained by continuous off-gas analysis during pulse experiments at different CO partial pressures

Figure 8 depicts the biomass specific rates for the three gaseous compounds as function of the CO% in the inlet gas. It can be seen that the biomass specific rates for CO and CO_2 increase linearly with the CO% in the inlet gas reaching a value of 89.1 $\pm$ 0.23 $mmol/gDCW/h$ for CO and 69.5 $\pm$ 0.70 $mmol/gDCW/h$ for CO_2. The linear increase of the biomass specific uptake rate indicates that the

maximum value has not been reached at 85% CO. On the other hand, hydrogen specific production rate constantly decreases until reaching a production rate of zero at 45% CO.The replicability of the results is very accurate since the standard deviation for CO and CO_2 is very low.

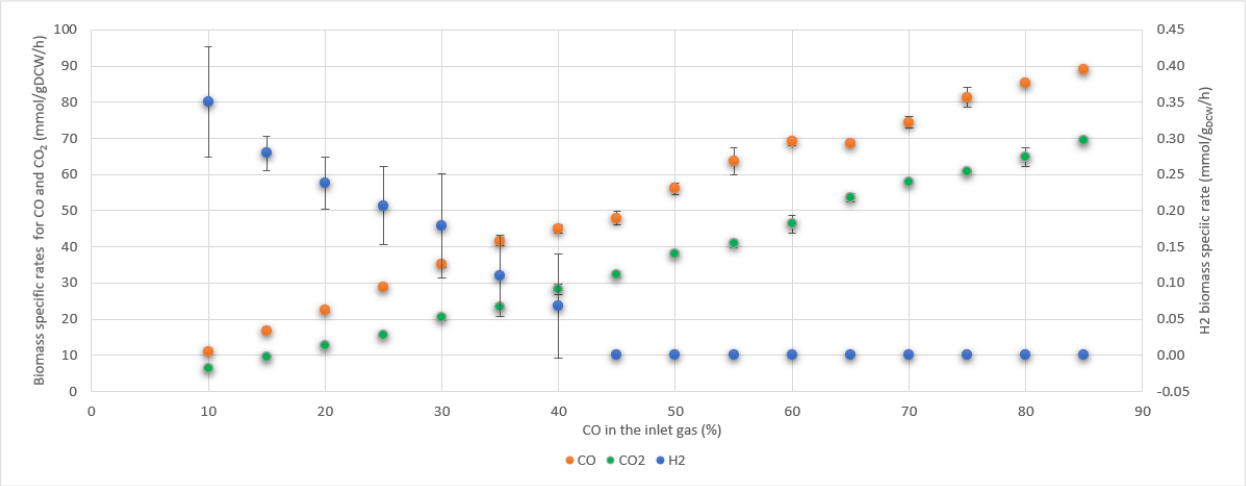

Figure 8: Biomass specific rates for CO (orange), CO_2 (green) and H_2 (blue) for different CO molar fractions in the inlet gas. The rates are given in mmol/gDCW/h. Hydrogen production rates are given in the right y-axis

Even if the maximum biomass specific uptake rate was not achieved, the growth rate can be determined according to Herbert-Pirt equation:

$$q_s = \frac{1}{Y_{X/S}^{max}} * \mu + m_s \tag{16}$$

When the growth rate is close to the maximum, the amount of substrate going for maintenance is negligible compared to the substrate consumed for biomass growth. Therefore, the maintenance term can be removed resulting in the following equation:

$$q_s = \frac{1}{Y_{X/S}^{max}} * \mu \tag{17}$$

For the maximum biomass yield, the biomass yield measured at steady state conditions (0.93 g_{DCW}/mol_{CO}) is used. This gives a growth rate of 0.083 h^{-1}, which is 16% higher than the thermodynamically derived maximum growth rate (0.064 and 0.063 h^{-1} for acetate and ethanol respectively / Section 2.7).

3.3 pH profile changes at higher CO partial pressures

During steady-state,it was seen that CO_2 off-gas profile was affected by the base addition. Therefore, it was decided to turn off the pH controller during the pulse experiments. The pH profile was monitored during the pulses and the pH change during the pulse experiments is depicted at Figure 9.

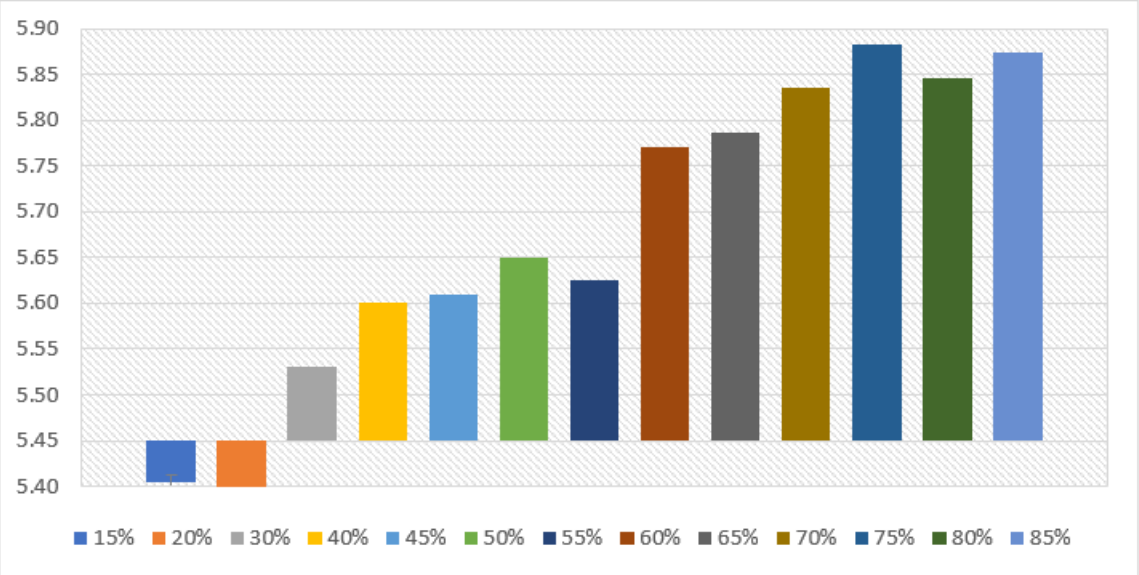

Figure 9: pH profile during pulse experiments for different CO % in the inlet gas. The pH before the start of the pulses is normalised to 5.45 for each case to compare .

It is observed that pH barely decreases from 5.45 to 5.40 for 15% and 20% CO, while after 30% of CO, pH increases up to 5.87. Since the pH controller is off and no base is added, the only compound that could increase the alkalinity of the cell broth is ethanol. Thus, there is the hypothesis that ethanol is formed during the pulse experiments at higher CO partial pressures, probably through acetate reduction.

To test this hypothesis, the product concentration of the samples before and after the pulses were compared. Ethanol can be produced through acetate reduction as shown in Figure 3. Acetate serves as the electron acceptor and it is reduced to ethanol. The only compound in the system which can be used as an electron donor is carbon monoxide which is oxidized to carbon dioxide. The redox reaction is displayed below:

$$2CO + CH_3COO^- + H_2O + H^+ \rightarrow CH_3CH_2OH + 2CO_2 \tag{18}$$

Figure 10 shows how the product concentrations change during the pulse experiments. It is seen that in most cases, acetate concentration decreases after the end of the pulse, while ethanol concentration increases, which could justify the pH increase.At 20, 70 and 75% though, the change in acetate concentration is positive. One way to explain that is the fact that the sample after the end of the pulse was taken when the off-gas values for CO and CO_2 were back at steady state levels which could affect the product concentration change. Nevertheless, the trend after 50% CO especially for ethanol formation is visible.

Furthermore, the standard deviations are very high at certain points. The main reason for that is the deviation of the concentrations during the pulse experiments as explained in Section 3.1. Moreover, in some cases, the concentration of acetate increases and in other cases it decreases for replicates of the same CO% in the inlet gas resulting to these high errors. Finally, it has to be mentioned that until the 45% CO pulse experiments, all the pulses were conducted at the same day so there is only one sample before and after the pulse. For this reason, no standard deviations exist for these points.

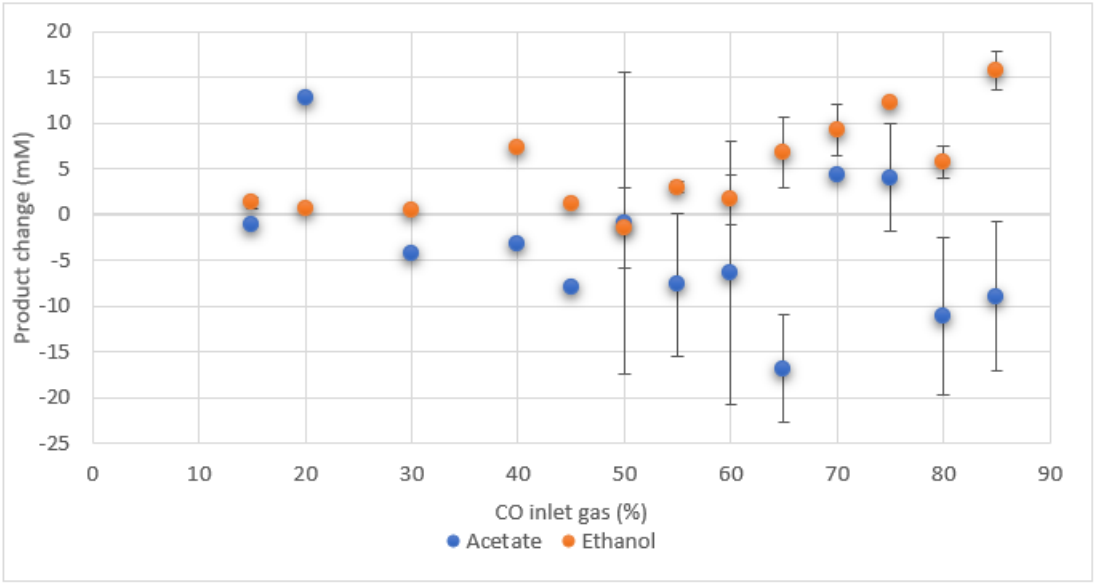

Figure 10: Acetate and ethanol concentration change in mM before and after the end of pulse experiments at different CO molar fractions with standard deviations.

3.4 Carbon dioxide to CO yield increases at higher CO molar fractions

The carbon dioxide production rate and biomass specific uptake rate were used to calculate the CO_2 to CO ratio (q_{CO2} / q_{CO}) during the pulse experiments, as shown in Figure 11.

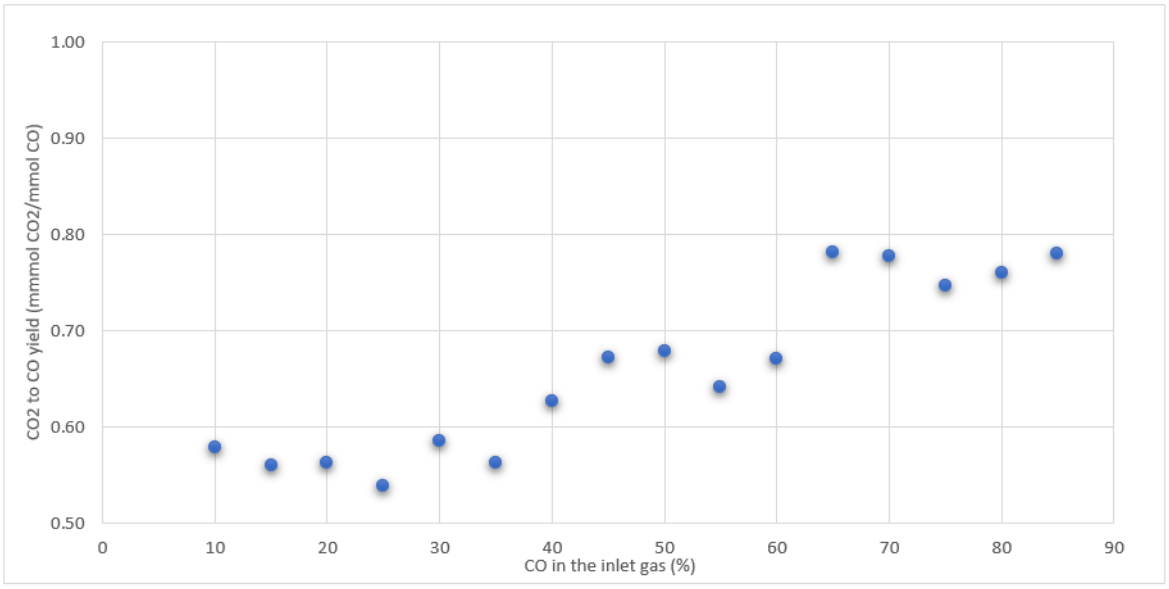

Figure 11: Carbon dioxide to CO ratio at different CO molar fractions.

It can be observed that the yield increases from 0.58 at steady-state conditions up to 0.78. The maximum theoretical yield for CO_2 according to Reactions 1 and 2 is just 0.67 when ethanol is the only product of CO fermentation. Reduction of acetate to ethanol, on the other hand, has a theoretical maximum CO_2 to CO ratio of 1 as shown in Reaction 18. This means that the yield of CO_2 probably increases due to a higher flux of acetate reduction at higher CO partial pressures. This hypothesis was tested by considering Reactions 1 and 18 and calculating the part of CO that it is dissipated to

each reaction based on the values shown in Figure 8. Assuming that the amount of CO consumed is distributed only among these two reactions, a solver was made using Microsoft Excel to calculate the percentage of CO that it is dissipated to each one. Next, the flux of acetate production and reduction were calculated using the stoichiometries of the two reactions.

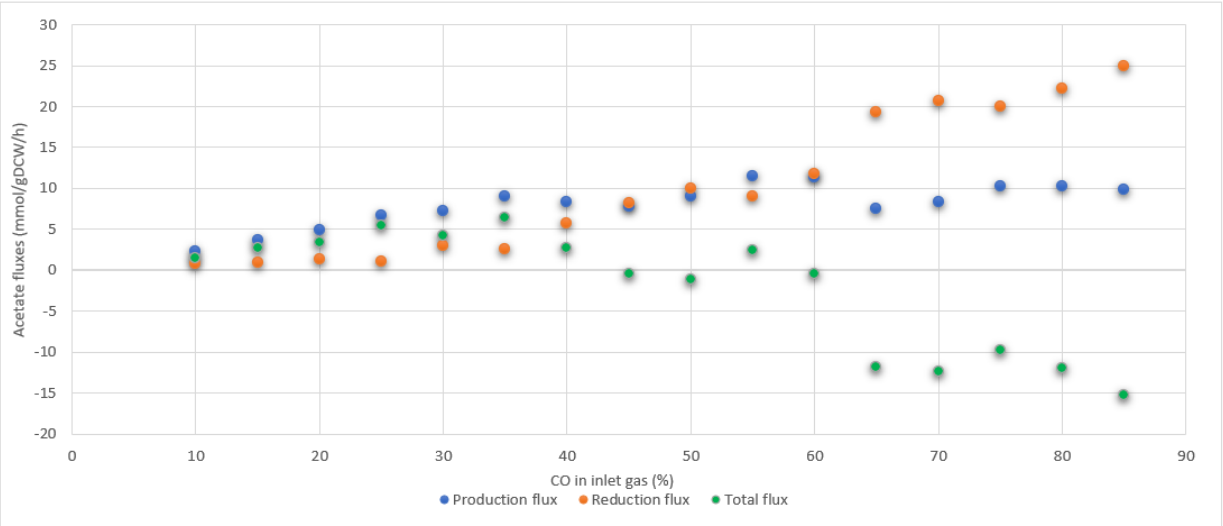

Figure 12: Acetate production (blue), reduction (orange) and total flux (green) at different CO molar fractions assuming that CO is distributed only among reactions 1 and 18

Figure 12 shows that as CO partial pressure in the inlet gas increases, both production and reduction fluxes increase, which can be explained by the higher consumption rate. However, after 45% of CO, the flux of acetate reduction becomes higher than the flux of acetate production. The difference between the two fluxes becomes even more visible after 65% of CO. Furthermore, acetate production rate remains constant at a flux of approximately 10 $mmol/g_{DCW}/h$ after 35% of CO. Finally, it has to be noticed that the total acetate flux estimated by the solver is lower (1.44 $mmol/g_{DCW}/h$) than the one observed during steady state (1.89 $mmol/g_{DCW}/h$). The exact opposite stands for ethanol which is produced at lower rates (0.21 and 0.84 $mmol/g_{DCW}/h$ for experimental and estimated results respectively).

3.5 Hydrogen gas profile during pulses

The pulse experiments also revealed interesting results related to the hydrogen gas production profile. Whenever a pulse was conducted, the hydrogen gas production decreased during the pulse until reaching the lowest value at the end of the pulse. When the pulse was over and the conditions were restored (CO 10% , N_2 90%), the partial pressure of H_2 started increasing again. Unlike CO and CO_2 partial pressures which were recovered after the end of the pulse and they reached the steady-state values, H_2 gas continued to be produced reaching more than 20% higher partial pressures compared to steady state. Furthermore, the time needed for the gas to go back to steady-state was much longer compared to CO and CO_2. Figure 13 depicts the off-gas profile for the three gaseous compounds as obtained by continuous off-gas analysis.

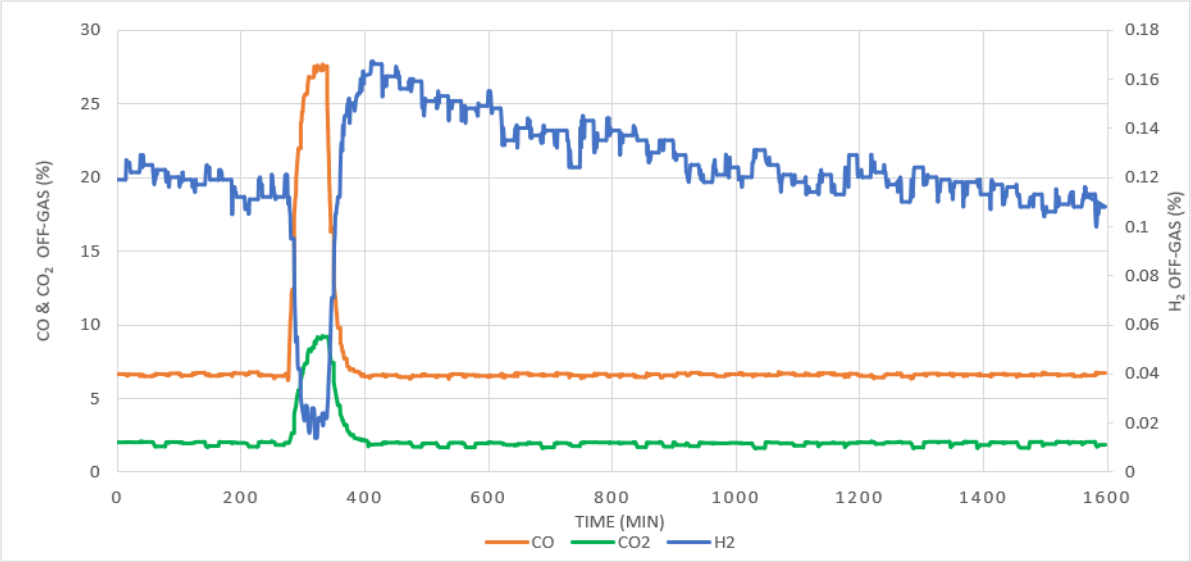

Figure 13: Off-gas profile for CO (orange),CO_2 (green) and H_2 (blue) as measured by continuous off-gas analysis during 40% CO pulse experiment. The pulse started around minute 270 and ended 60 minutes later. H_2 off-gas profile is given in the right y-axis

4 Discussion

4.1 Absence of yeast extract does not affect the microbial growth

Three different steady states were achieved while different feed mineral media were used to evaluate the effect of yeast extract on the concentration of the products. The results showed that the absense of yeast extract in the feed mineral medium did not have an impact on biomass growth, as the same biomass concentration was achieved in both cases (SS1 and SS2). Acetate concentration was also very comparable, however ethanol concentration was significantly lower (0.61 ± 0.13 g/L for SS1 and 0.41 ± 0.03 g/L for SS2). These results do not agree with the study reported by Barik et al. [36], who found that the absence of yeast extract improved by three times the ethanol/acetate ratio in a *Clostridium* species, which they were not able to identify at that time. Same results have also been reported by Phillips et al. [37], who have studied syngas fermentation in *Clostridium Ljungdahlii* and they have found out that absence of yeast extract and six times lower B-vitamin concentration resulted to higher ethanol production but lower cell growth, which probably occured due to the B-vitamin shortage. In this study, when yeast extract was present, the ethanol to acetate ratio was 0.15 g/g (SS1) while this ratio dropped to 0.08 g/g (SS2) when the chemically defined medium was used.According to Abubackar et al. [38], the decrease in ethanol production may be related to the absence of vitamin B12 that is contained in yeast extract. Nevertheless, the chemically defined medium contained this vitamin, so this should not be the reason why the formation of ethanol decreases.

The third steady state was achieved at a higher agitation speed and lower working volume resulting in a higher mass transfer capacity and thus a higher biomass specific uptake rate. This was also accompanied by a higher biomass concentration compared to the other two steady states as well as a notable acetate concentration increase. Surprisingly, though, the ethanol concentration slightly increased with the ethanol to acetate ratio being 0.085 g/g, almost equal to the ratio observed in SS2. Increased acetate production with higher biomass levels could imply that acetate is associated with growth and ethanol is not [36]. However, this hypothesis has been questioned by newer studies [4]. One logical explanation regarding the lower ethanol concentration is the composition of yeast extract. Yeast extract contains all the necessary nutrients, vitamins and trace elements to boost the microbial growth [38]. Thus, the use of yeast extract in the mineral medium could result in higher levels of acetyl-CoA, which could be further reduced to ethanol via the indirect pathway.

4.2 Pulse experiments can be efficiently used to derive the maximum substrate uptake rate

The results obtained by the pulse experiments verified the hypothesis that the gas-liquid mass transfer rate is the limiting step in the fermentation since the biomass specific uptake rate continued increasing linearly until the end of the feeding disturbances at 85% CO in the inlet gas. The high replicability of the results show that this experimental design is an accurate way to estimate the kinetic parameters of a microorganism experimentally. Even though this technique has been used before by Sipkema et al. [21] to extract the kinetic parameters of two aerobic microorganisms (*Methylosinus trichosporium* and *Burkholderia (Pseudomonas) cepacia*) by increasing the oxygen supply, it has not been reported yet a similar study for the determination of the maximum biomass specific uptake rate and maximum growth rate in acetogenic bacteria. The pulse experiments can thus provide novel information for the estimation of the kinetic parameters of *C.autoethanogenum*. The biomass specific uptake rate of 89.1 ± 0.23 $mmol/g_{DCW}/h$ achieved during the pulse experiments is 30% higher than the highest biomass specific CO uptake rate (70 $mmol/g_{DCW}/h$) reported so far in literature by Lima et al. [23]. However, the calculated growth rate ($0.083h^{-1}$) is lower than the value reported in their study (0.116 h^{-1}) indicating that the biomass yield reached at steady state is not the maximum that the cells can reach. Indeed, the authors of this paper have obtained a biomass yield of 1.66 g_{DCW}/mol_{CO}, which is 80% higher than the biomass yield obtained in this study. Using the biomass yield that the same authors

obtained, a growth rate of 0.148 h^{-1} is derived at a biomass specific uptake rate of 89.1 $mmol/g_{DCW}/h$ according to Equation 17.

Several studies have also been conducted to derive the kinetic parameters of acetogens. Mohammadi et al. [39] have studied the kinetic parameters of *Clostridium Ljungdahlii* in pressurized batch bottles without pH fixation using syngas. Using a dual-substrate kinetic model, the authors derived a maximum growth rate of 0.195 h^{-1} but their maximum biomass specific CO uptake rate was only 34.37 $mmol/g_{DCW}/h$, almost 3 times lower than the value reported in this study. The maximum biomass yield given these numbers is 5.67 g_{DCW}/mol_{CO} which is extremely high, indicating that the estimation of the kinetic parameters in batch fermentation for gas-liquid mass transfer systems leads to questionable results. A dynamic model has also been published by Medeiros et al. [17] using experimental data for continuous cultivation of *C. Ljungdahlii* on syngas. The same authors have derived a maximum CO uptake rate of 46.3 $mmol/g_{DCW}/h$, which is almost 50% lower that the uptake rate obtained from the pulse experiments. Compared to these studies, pulse experiments provide the advantage of calculating the key kinetic parameters of a microorganism directly without the requirement of fitting experimental data to a model that can be based on assumptions which can lead to high variability.

4.3 Comparison of experimental and theoretical biomass specific uptake rate

The theoretical estimation of the kinetic parameters using the thermodynamic approach resulted in a maximum biomass specific CO uptake rate of 60.0 $mmol_{CO}/g_{DCW}/h$ and 65.0 $mmol_{CO}/g_{DCW}/h$ for acetate and ethanol respectively (Section 2.7). These values are approximately 40% lower than the experimental value of 89.1 $\pm$ 0.23 $mmol/g_{DCW}/h$. The difference between the results is related to the assumptions made to derive the kinetic parameters. Specifically, the assumption of the maximum electron capacity in catabolism can strongly affect μ_{max} as shown in Equation C.2 and therefore q_s^{max}. This value is valid when the electrons are transferred from an electron donor to an external electron acceptor via the electron transport chain. In a fermentation,there is no terminal electron acceptor and the electrons are relocated to end up in the catabolic products [40]. Therefore, this assumption could explain why the thermodynamically estimated q_s^{max} is lower than the experimental value. This analysis also provided knowledge regarding the maximum biomass yield that the microorganism can achieve. The use of the Gibbs energy dissipation method resulted in a maximum biomass yield of 1.35 g_{DCW}/mol_{CO} and 1.24 g_{DCW}/mol_{CO} for acetate and ethanol respectively, while the biomass yields estimated from the ATP balancing method were even higher (2.05 g_{DCW}/mol_{CO} and 1.89 g_{DCW}/mol_{CO} for acetate and ethanol). Both of these methods lead to higher biomass yields than the one reached at steady state (0.93 $\pm$ 0.06 g_{DCW}/mol_{CO}). The higher yields using the ATP balancing method are closely related to the λ_{cat} values obtained using this method. A lower λ_{cat} means that the catabolism has to run less times to produce one Cmole of biomass resulting in a higher biomass yield. The biomass yield of 1.66 g_{DCW}/mol_{CO} reported by Lima et al. [17] is between this biomass yield range. Therefore, the growth rate of 0.148 h^{-1} estimated using the biomass yield reported by these authors could be close to the maximum.

4.4 Acetate is reduced to ethanol so that the cells can regulate their metabolism

During the pulse experiments, it was seen that the CO_2 to CO ratio increased, which was related to ethanol production through acetate reduction. Supplying more CO leads to higher consumption rates and thus higher growth rates. Faster growth demands more energy for biomass synthesis and product formation. Meanwhile, ethanol production rate also increased according to Figure 10. Elevated ethanol production at increased growth rates has also been reported in a different study [23]. Higher concentration of reduced products results in an increasing demand for reduced ferredoxin [41]. This might explain why hydrogen formation completely stops after 45% of CO. The redox power demands for ATP formation and ethanol reduction are high enough that no reduced ferredoxin can be used to produce hydrogen through the HytA-E/FdhA complex. Zero hydrogen production after 45% of CO

agrees with the data reported by other authors who performed CO fermentation using 60% of CO in the ingas mixture [22, 23]. CO inhibition is not probably responsible for the hydrogen production rate decrease given the fact that the fermentation continues to be mass-transfer limited and thus CO limited.

The main question, however, is why the reduction of acetate to ethanol continues.The AOR enzyme is in direct competition with the Rnf complex since reduced ferredoxin is required in both of these reactions. As growth rate increases and more biomass is formed, acetate concentration also increases. As extracellular acetate concentration increases, more undissociated acid can penetrate the cell and leak protons lowering the intracellular pH [42]. These protons cannot be used for the synthesis of ATP because only the protons produced through the Rnf complex can be utilised to generate ATP [43]. Valgepea et al. [15] have performed a metabolomics analysis and have found out that this uncoupling of the proton motive force increases the ATP requirements for maintenance and therefore the total ATP requirements. By reducing acetate to ethanol, this phenomenon can be prevented. However, more energy is required which is provided by the oxidation of CO to CO_2 [15], leading to a higher CO_2 to CO ratio.

The estimation of the acetate production and reduction fluxes based on the q-rates for CO and CO_2 showed that the flux of acetate production reaches a plateau of approximately 10 $mmol/g_{DCW}/h$ after 35% of CO in the inlet gas. This constant flux could indicate that there is a reaction inside the WLP which is limiting. This limitation could potentially occur due to the increased redox demands for ATP and ethanol production. The oxidation of CO to CO_2, which provides the reduced ferredoxin that the cells need to form ATP and produce ethanol, diminishes the available carbon supply for the WLP, thus limiting the synthesis of acetyl-CoA. Amador-Noguez et al. [44] have observed a drop in acetyl-CoA intracellular concentration during the switch from the acetogenic to the solventogenic phase in *Clostridium acetobutylicum*. Same results have been reported stating that the higher ATP requirements at higher biomass concentrations led to the depletion of the acetyl-CoA pool and the loss of CO uptake and eventually the collapse of the metabolism [15]. Mahamkali et al.[41] have also reported oscillations in CA cultures by increasing the agitation speed. The authors have suggested that an arrest of the WLP and a deregulation of the cells occurs due to a loss of the AOR driving force as ethanol concentration increases. These observations can provide significant insight regarding the outcome of the pulse experiments if longer time periods are tested.

4.5 Hydrogen gas is only produced under a mass transfer limited regime.

Steady state data revealed that hydrogen gas is produced in SS1 and SS3 at very low amounts even though it was not anticipated since the experimental results reported by other authors [22, 23, 14], who also studied the fermentation of *C.autoethanogenum* using CO as the only carbon and energy source, did not reveal any H_2 formation.
CO inhibits the activity of the hydrogenases, enzymes that catalyze the formation or uptake of H_2, at relatively low concentrations [45]. Moreover, Wang et al. [24] in 2013 discovered that CA cultures grown on CO possess a NADP and ferredoxin dependent electron bifurcating [Fe-Fe] hydrogenase which forms a complex with formate dehydrogenase. According to their study, this complex, known as HytA-E/FdhA, can catalyze the formation of hydrogen gas from reduced ferredoxin (Fd^{2-}) and NADPH as well as the reduction of CO_2 to formate with the two aforementioned electron carriers. Under physiological conditions, this reaction is thermodynamically unfeasible since the ΔG^0 is +21 kJ/mol [24]. However, the average partial pressure of hydrogen during steady state is very low for SS1 (0.002 atm) and SS3 (0.001 atm) which can result in a negative Gibbs energy change.Since fermentation operates under a mass transfer limited regime, the residual concentration of CO is very close to zero. Therefore, under these conditions CO may not inhibit the hydrogenases which produce hydrogen gas at low rates.

In Section 3.4 it was mentioned that the production rate of ethanol for SS3 is lower than expected given the biomass specific uptake rate and CO_2 specific production rate observed. On the other hand, the production rate of acetate was higher than it should be.Thus, the fact that cells waste energy to produce H_2 and not to make ethanol via acetate reduction raises questions. Even more surprising is the fact that ethanol reduction through acetate is more thermodynamically feasible than hydrogen production under physiological conditions (ΔG^0 of -93 kJ/mol for a redox potential of -320 mV for $NAD+/NADH$ and -450 mV for Fd_{ox}/Fd^{2-} [8]). Thus, this observation requires further study. One possible explanation about this is that the production of ethanol via the AOR and Adh enzymes requires more redox power than hydrogen production. One mole of ethanol produced requires one mole of reduced ferredoxin and NADH. On the other hand, one mole of hydrogen gas requires 0.5 moles of reduced ferredoxin and NADPH, while 0.25 moles of reduced ferredoxin are required to produce 0.5 moles of NADPH through the Nfn complex. Therefore, one mole of hydrogen requires 0.75 moles of reduced ferredoxin instead of one mole required for ethanol production. This hydrogen-over-ethanol selection leaves more reduced ferredoxin available for the Rnf complex, creating a higher proton flux for ATP generation.

4.6 Hydrogen gas overproduction after the pulses might be related to an overreduction of the electron carriers.

After the end of the pulse experiments, an overproduction of hydrogen gas was exhibited. It is possible that hydrogen gas production has to do with the metabolic regulation of the cells. Wang et al. [24] have conducted a specific activity analysis in CA cultures grown on syngas and have discovered that formate dehydrogenase is also inhibited by CO at low concentrations. Their analysis showed that the reduction of ferredoxin with CO catalyzed by CODH in the first step of the Wood-Ljungdahl pathway is very favorable which makes the reoxidation of the electron carrier the limiting step. As a result, a lower flux of ferredoxin reoxidation would slow down the CO oxidation to CO_2 leading to CO accumulation and inhibition of the formate hydrogenases. In that case, CO will be oxidized by reducing ferredoxin, NAD^+ and $NADP^+$ since it has a more negative redox potential ($E'_o = -520mv$ for CO) resulting in an overreduction of the electron carriers deregulating cell metabolism. In extreme conditions like these, the H cluster of [Fe-Fe] hydrogenase that is bound to CO can be released and produce H_2 very fast despite high CO concentrations. This option is realistic considering the reduced ferredoxin elevated demands for ATP and ethanol formation during the pulse experiment, which could drop significantly the Fd_{ox}/Fd^{2-} ratio and thus slow down the CO oxidation to CO_2 resulting in an overreduction of the redox carriers.

Overproduction of hydrogen gas could also be attributed to ethanol oxidation back to acetate once the pulse is over. When ethanol is oxidized to acetaldehyde, one mole of NADH is released while further oxidation to acetate produces one mole of reduced ferredoxin. However, the only way for the cells to produce equimolar amounts of reduced ferredoxin and NADH and close the metabolites balance is by catalyzing the oxidation of NADH to NAD^+ to produce reduced ferredoxin which is the reversed reaction in the Rnf complex. NADH can then be balanced in the Nfn complex which produces NADPH. NADPH can finally be oxidized in the HytA-E/FdhA with reduced ferredoxin to produce H_2 gas. However, this option is questionable given the fact that the cells would generate less ATP since protons would have to be invested to produce hydrogen gas, without even considering if the reversed reaction is thermodynamically feasible.

5 Conclusions

The main key conclusions of this study are summarized below:

- The absence of yeast extract from the mineral medium showed no change in the biomass and acetate concentration levels but resulted in a lower ethanol production, which is attributed to the yeast extract composition
- Pulse experiments are a novel method to derive the key kinetic parameters of a microorganism. During these experiments, the biomass specific CO uptake rate achieved (89.1 $mmol_{CO}/g_{DCW}/h$) was higher than any other value reported in literature.
- Fermentation continues to be mass transfer limited at 85% of CO in the inlet gas since biomass specific CO uptake rate increased linearly until that point.
- The calculated growth rate of 0.083 h^{-1} is lower compared to literature showing that the biomass yield reached during steady state is lower than the maximum biomass yield that the cells could achieve.
- The increase of the CO molar fraction in the inlet gas revealed an increase in the CO_2 to CO ratio which was related to acetate reduction to ethanol so that the cells can regulate their metabolism and maintain the ATP requirements.
- A limitation of acetyl-CoA formation due to increased CO to CO_2 oxidation results in a constant biomass specific acetate production rate after 35% of CO.
- *C.autoethanogenum* can produce trace amounts of hydrogen gas via the [Fe-Fe] electron bifurcating hydrogenase when the culture is CO limited.
- Hydrogen gas overproduction after the end of the pulse occurs due to the overreduction of the redox carriers.

6 Recommendations

The pulse experiments design showed that this method can be used to calculate the maximum biomass specific substrate uptake rate. However, the maximum value was not reached. Therefore, the next step would be the increase of CO in the inlet gas up to 100% to see whether the maximum uptake rate can be achieved.Furthermore, dilution rates higher than 0.116 h^{-1} (which is the dilution rate tested by Lima et al. [23] could be tested to find out whether the maximum growth could be achieved and how much the product spectrum changes compared to the steady state achieved at 0.01 h^{-1}. Nevertheless, higher agitation speeds and CO partial pressure in the inlet gas would be required in order to ensure that the substrate is enough for the cells to grow. Furthermore, it would be interesting to identify the dilution rate at which hydrogen production stops and compare it with the literature data reported for CO fermentation. The absence of yeast extract at a dilution rate of 0.008 h^{-1} affected the ethanol production rate which was lower compared to the yeast extract containing medium. Therefore, it would be interesting to study the effect of the absence of yeast extract at higher dilution rates to see whether the results agree with the studies reported so far. The construction of a metabolic model could also provide insight into the results obtained by the pulse experiments. Specifically, the model could show whether the constant acetate production flux is related to a limitation in the acetyl-CoA formation as well as indicate the mechanism behind the hydrogen gas overproduction. An intracellular metabolome analysis could also be performed to compare the results with the metabolic model. Finally, the co-metabolism of CO and H_2 could by studied. Under a CO limited system, H_2 could donate the electrons for the WLP resulting in a lower dissipation of carbon as CO_2 which could enhance the production of reduced products such as ethanol as reported by Valgepea et al. [22].

Acknowledgement

During my master thesis project, I received a lot of help from people who I would like to thank.

First of all, I would like to thank my daily supervisor, Maxim Allaart, who was always there to support me, guide me and help me manage my enormous stress levels. Her constructive feedback was significant for the continuation of this project. I really enjoyed the long discussions we had about the interpretation of the results.

Besides my daily supervisor, I would like to thank Robbert Kleerebezem, David Weissbrodt and Adrie Straathof, for participating in my thesis committee. Robbert Kleerebezem was also my main supervisor during this project. I really enjoyed the biweekly meetings we had, from which I learned a lot and I always received new suggestions about how to proceed during the project.

Furthermore, I would like to thank Marina Perdigão Elisiário for the nice discussions we had at the lab and her assistance regarding the lab set up. I could not forget the lab technicians Dirk, Song and Christiaan who were always there to provide their help whenever I needed it.

A special thanks to the EBT group for creating a pleasant environment.Everybody has been very helpful. I learned many things from the weekly seminars we had.

Last but not least, I would like to thank my family and friends who have always supported me during my studies and especially during my master thesis.

Bibliography

[1] METGroup Countries. *When will fossil fuels run out.* 2021. URL: https://group.met.com/en/mind-the-fyouture/mindthefyouture/when-will-fossil-fuels-run-out (visited on 04/15/2021).

[2] Mamatha Devarapalli and Hasan K Atiyeh. "A review of conversion processes for bioethanol production with a focus on syngas fermentation". In: *Biofuel Research Journal* 2.3 (2015), pp. 268–280.

[3] Haris Nalakath Abubackar, Marı´a C Veiga, and Christian Kennes. "Biological conversion of carbon monoxide: rich syngas or waste gases to bioethanol". In: *Biofuels, Bioproducts and Biorefining* 5.1 (2011), pp. 93–114.

[4] Jacqueline L Cotter, Mari S Chinn, and Amy M Grunden. "Influence of process parameters on growth of Clostridium ljungdahlii and Clostridium autoethanogenum on synthesis gas". In: *Enzyme and Microbial Technology* 44.5 (2009), pp. 281–288.

[5] M Gupta and JJ Spivey. "Chapter 5-Catalytic Processes for the Production of Clean Fuels". In: *New and Future Developments in Catalysis, Suib, SL, Ed. Elsevier: Amsterdam* (2013), pp. 87–126.

[6] Habibollah Younesi, Ghasem Najafpour, and Abdul Rahman Mohamed. "Liquid fuel production from synthesis gas via fermentation process in a continuous tank bioreactor (CSTBR) using Clostridium ljungdahlii". In: *Iranian Journal of Biotechnology* 4.1 (2003), pp. 45–53.

[7] Stephen W Ragsdale and Elizabeth Pierce. "Acetogenesis and the Wood–Ljungdahl pathway of CO2 fixation". In: *Biochimica et Biophysica Acta (BBA)-Proteins and Proteomics* 1784.12 (2008), pp. 1873–1898.

[8] Christian Öppinger, Florian Kremp, and Volker Müller. "Is reduced ferredoxin the physiological electron donor for MetVF-type methylenetetrahydrofolate reductases in acetogenesis? A hypothesis". In: *International Microbiology* 25.1 (2022), pp. 75–88.

[9] Johanna Mock et al. "Energy conservation associated with ethanol formation from H2 and CO2 in Clostridium autoethanogenum involving electron bifurcation". In: *Journal of bacteriology* 197.18 (2015), pp. 2965–2980.

[10] Johannes Bertsch and Volker Müller. "Bioenergetic constraints for conversion of syngas to biofuels in acetogenic bacteria". In: *Biotechnology for biofuels* 8.1 (2015), pp. 1–12.

[11] Kai Schuchmann and Volker Müller. "Autotrophy at the thermodynamic limit of life: a model for energy conservation in acetogenic bacteria". In: *Nature Reviews Microbiology* 12.12 (2014), pp. 809–821.

[12] JL Vega et al. "The biological production of ethanol from synthesis gas". In: *Applied Biochemistry and Biotechnology* 20.1 (1989), pp. 781–797.

[13] Alba Infantes, Michaela Kugel, and Anke Neumann. "Effect of cysteine, yeast extract, pH regulation and gas flow on acetate and ethanol formation and growth profiles of clostridium ljungdahlii syngas fermentation". In: *BioRxiv* (2020).

[14] Haris Nalakath Abubackar, Marı´a C Veiga, and Christian Kennes. "Carbon monoxide fermentation to ethanol by Clostridium autoethanogenum in a bioreactor with no accumulation of acetic acid". In: *Bioresource technology* 186 (2015), pp. 122–127.

[15] Kaspar Valgepea et al. "Maintenance of ATP homeostasis triggers metabolic shifts in gas-fermenting acetogens". In: *Cell systems* 4.5 (2017), pp. 505–515.

[16] James K Heffernan et al. "Enhancing CO2-valorization using Clostridium autoethanogenum for sustainable fuel and chemicals production". In: *Frontiers in bioengineering and biotechnology* 8 (2020), p. 204.

[17] Elisa M de Medeiros et al. "Dynamic modeling of syngas fermentation in a continuous stirred-tank reactor: Multi-response parameter estimation and process optimization". In: *Biotechnology and Bioengineering* 116.10 (2019), pp. 2473–2487.

[18] Rolf Sander. "Compilation of Henry's law constants (version 4.0) for water as solvent". In: *Atmospheric Chemistry and Physics* 15.8 (2015), pp. 4399–4981.

[19] Andrew J Ungerman and Theodore J Heindel. "Carbon monoxide mass transfer for syngas fermentation in a stirred tank reactor with dual impeller configurations". In: *Biotechnology progress* 23.3 (2007), pp. 613–620.

[20] Alan H Scragg. *Bioreactors in biotechnology: a practical approach.* 1991.

[21] EM Sipkema et al. "Experimental pulse technique for the study of microbial kinetics in continuous culture". In: *Journal of Biotechnology* 64.2-3 (1998), pp. 159–176.

[22] Kaspar Valgepea et al. "H2 drives metabolic rearrangements in gas-fermenting Clostridium autoethanogenum". In: *Biotechnology for biofuels* 11.1 (2018), pp. 1–15.

[23] Lorena Azevedo de Lima et al. "Faster growth enhances low carbon fuel and chemical production through gas fermentation". In: *Frontiers in Bioengineering and Biotechnology* 10 (2022).

[24] Shuning Wang et al. "NADP-specific electron-bifurcating [FeFe]-hydrogenase in a functional complex with formate dehydrogenase in Clostridium autoethanogenum grown on CO". In: *Journal of bacteriology* 195.19 (2013), pp. 4373–4386.

[25] V Müller and A Wiechmann. "Synthesis of acetyl-CoA from carbon dioxide in acetogenic bacteria". In: *Biogenesis of Fatty Acids, Lipids and Membranes; Geiger, O., Ed* (2017), pp. 1–18.

[26] Martijn Diender, Alfons JM Stams, and Diana Z Sousa. "Production of medium-chain fatty acids and higher alcohols by a synthetic co-culture grown on carbon monoxide or syngas". In: *Biotechnology for biofuels* 9.1 (2016), pp. 1–11.

[27] Felix Garcia-Ochoa and Emilio Gomez. "Bioreactor scale-up and oxygen transfer rate in microbial processes: an overview". In: *Biotechnology advances* 27.2 (2009), pp. 153–176.

[28] Edward Lansing Cussler and Edward Lansing Cussler. *Diffusion: mass transfer in fluid systems.* Cambridge university press, 2009.

[29] Charlène Thobie et al. "Global characterization of hydrodynamics and gas-liquid mass transfer in a thin-gap bubble column intended for microalgae cultivation". In: *Chemical Engineering and Processing: Process Intensification* 122 (2017), pp. 76–89.

[30] Hai-Feng Zhu et al. "Energy conservation and carbon flux distribution during fermentation of CO or H2/CO2 by Clostridium ljungdahlii". In: *Frontiers in microbiology* 11 (2020), p. 416.

[31] JJ Heijnen and JP Van Dijken. "In search of a thermodynamic description of biomass yields for the chemotrophic growth of microorganisms". In: *Biotechnology and Bioengineering* 39.8 (1992), pp. 833–858.

[32] Joseph J Heijnen and Robbert Kleerebezem. "Bioenergetics of microbial growth". In: *Encyclopedia of bioprocess technology: Fermentation, biocatalysis, and bioseparation* 1 (1999), pp. 267–291.

[33] L Tijhuis, Mark CM Van Loosdrecht, and JJv Heijnen. "A thermodynamically based correlation for maintenance Gibbs energy requirements in aerobic and anaerobic chemotrophic growth". In: *Biotechnology and bioengineering* 42.4 (1993), pp. 509–519.

[34] Robbert Kleerebezem. *Thermodynamics.* University Lecture. 2020.

[35] IK Stoll et al. "Fermentation of H_2 and CO_2 with Clostridium ljungdahlii at Elevated Process Pressure–First Experimental Results". In: *Chemical Engineering Transactions* 64 (2018), pp. 151–156.

[36] S Barik et al. "Biological production of alcohols from coal through indirect liquefaction". In: *Applied biochemistry and biotechnology* 18.1 (1988), pp. 363–378.

[37] JR Phillips et al. "Biological production of ethanol from coal synthesis gas". In: *Applied biochemistry and biotechnology* 39.1 (1993), pp. 559–571.

[38] Haris Nalakath Abubackar, Marı´a C Veiga, and Christian Kennes. "Ethanol and acetic acid production from carbon monoxide in a Clostridium strain in batch and continuous gas-fed bioreactors". In: *International journal of environmental research and public health* 12.1 (2015), pp. 1029–1043.

[39] Maedeh Mohammadi et al. "Kinetic studies on fermentative production of biofuel from synthesis gas using Clostridium ljungdahlii". In: *The Scientific World Journal* 2014 (2014).

[40] David G Weissbrodt et al. "Basic microbiology and metabolism". In: *Biological Wastewater Treatment: Principles, Modelling and Design* (2020).

[41] Vishnuvardhan Mahamkali et al. "Redox controls metabolic robustness in the gas-fermenting acetogen Clostridium autoethanogenum". In: *Proceedings of the National Academy of Sciences* 117.23 (2020), pp. 13168–13175.

[42] Maedeh Mohammadi et al. "Bioconversion of synthesis gas to second generation biofuels: A review". In: *Renewable and Sustainable Energy Reviews* 15.9 (2011), pp. 4255–4273.

[43] Maria Hermann et al. "Electron availability in CO2, CO and H2 mixtures constrains flux distribution, energy management and product formation in Clostridium ljungdahlii". In: *Microbial Biotechnology* 13.6 (2020), pp. 1831–1846.

[44] Daniel Amador-Noguez et al. "Metabolome remodeling during the acidogenic-solventogenic transition in Clostridium acetobutylicum". In: *Applied and environmental microbiology* 77.22 (2011), pp. 7984–7997.

[45] Seigo Shima and Rudolf K Thauer. "A third type of hydrogenase catalyzing H2 activation". In: *The chemical record* 7.1 (2007), pp. 37–46.

A Appendix

A.1 Protocol for TSS/VSS measurements

- Weight 2x empty 50 mL tube
- Fill each tube with approximately 50 mL effluent
- Weight 2x filled 50 mL tubes
- Spin off 2x 50 mL tubes for 25 minutes at 4200 x rpm in centrifuge at 10°C
- Get supernatant off
- Resuspend the pellets in 20 mL Milli-Q and spin down again
- Get supernatant off
- Dissolve pellet in 5 mL Milli-Q
- Weight 2 empty pre-ashed cups
- Get 2x 5mL dissolved pellet into empty cup
- Put in 105°C oven at least overnight
- Weight dry weight matter in cup
- Ash at 550°C for 3 hours
- Leave the samples in the desiccator cabinet for 3 minutes
- Weight ash in cup

Then, the biomass concentration in dry cell weight per liter is calculated as follows:

$$g_{DCW}/L = TSS * (1 - Ash\%) \tag{A.1}$$

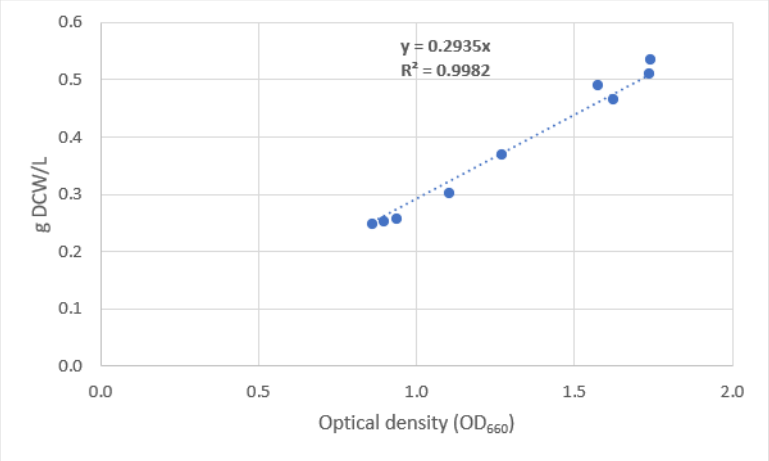

Figure A.1: Correlation between optical density at 660 nm and biomass concentration in dry cell weight per liter for *C.autoethanogenum* grown on CO

A.2 Protocol for CO fermentation

- Start with 100 ml/min of gas flow rate and 10% CO. Starting with low stirring speed will reduce the risk of toxifying the cells. High mass transfer rate can lead to CO accumulation in the liquid at low biomass concentrations and cell death
- Check daily the optical density. If OD does not increase, consider of increasing the stirring speed or the CO in the inlet gas (from 100 to 150 rpm and from 10% to 15% CO)
- After 72 hours of cultivation, increase the stirring speed to 200 rpm
- 24 hours later, increase the CO in the inlet gas at 20%
- Increase stirring speed every 24 hours by 100 rpm if OD increases, otherwise every 48 hours until reaching the conditions for chemostat.

B Appendix

B.1 Mass transfer coefficient kla at different agitation speeds

Table B.1: Mass transfer coefficient kla for CO at different agitation speeds

Stirring speed (rpm)	kla for CO at 37°C
300	8.17
500	22.41
600	35.82
700	24.54
800	20.18

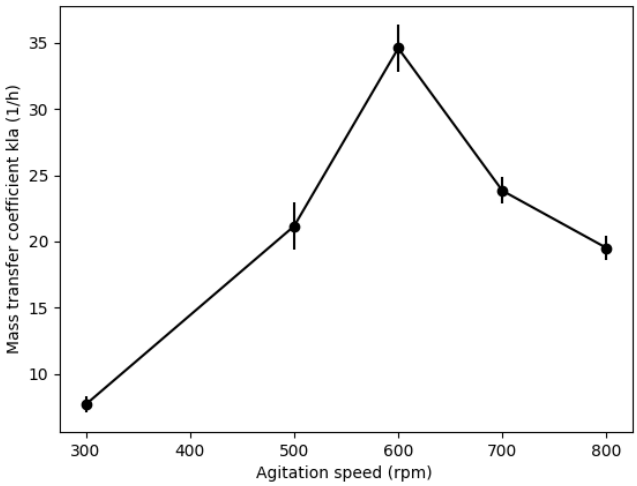

Figure B.1: Mass transfer coefficient for CO at different agitation speeds

B.2 Steady state data for the three chemostats

Table B.2: Steady state growth characteristics for three different chemostat cultures with standard deviations. Biomass specific rates are given in mmol/gDCW/h. The gas flow rate at every case is 100 ml/min.

Parameters	SS1	SS2	SS3
Biomass concentration (gDCW/L)	0.39 ± 0.01	0.41 ± 0.02	0.53 ± 0.02
q_{co}	8.61 ± 0.68	15.9 ± 0.60	10.8 ± 0.54
q_{co2}	6.12 ± 0.48	4.9 ± 0.18	6.26 ± 0.35
q_{H2}	0.66 ± 0.05	0	0.35 ± 0.08
$q_{acetate}$	1.67 ± 0.19	1.68 ± 0.12	1.89 ± 0.28
$q_{ethanol}$	0.32 ± 0.06	0.18 ±0.02	0.21 ± 0.03
Biomass yield (gDCW/mol)	0.93 ± 0.07	0.50 ± 0.02	0.93 ± 0.06
$C_{ethanol}$ (g/L)	0.69 ± 0.13	0.41 ± 0.03	0.51± 0.09
$C_{acetate}$ (g/L)	4.65 ± 0.46	5.12 ± 0.25	5.95 ± 0.93

B.3 Carbon and electron recoveries for the three steady-states

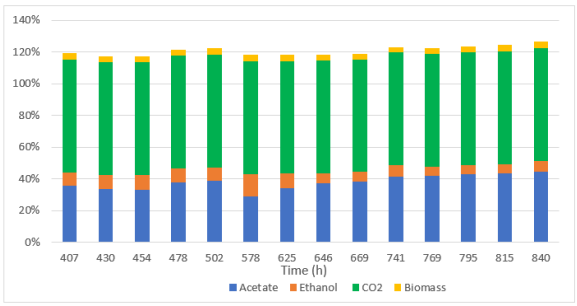

(a) C- balance

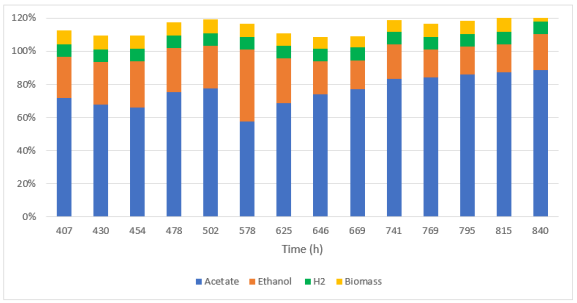

(b) e-balance

Figure B.2: Carbon (a) and electron balance (b) for first steady state

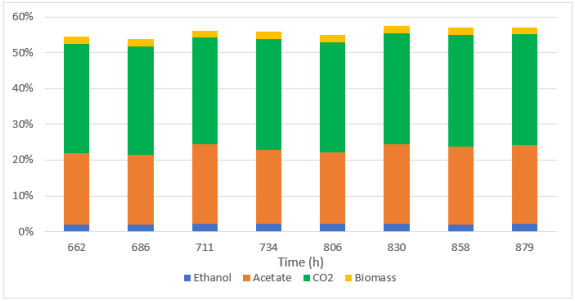

(a) C- balance

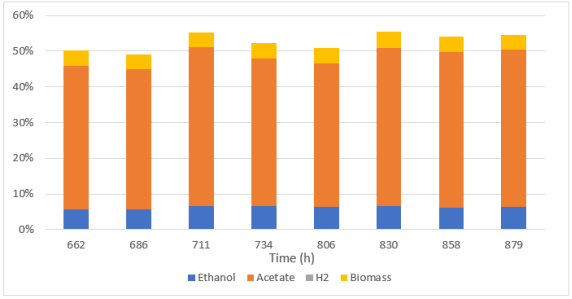

(b) e-balance

Figure B.3: Carbon (a) and electron balance (b) for second steady state

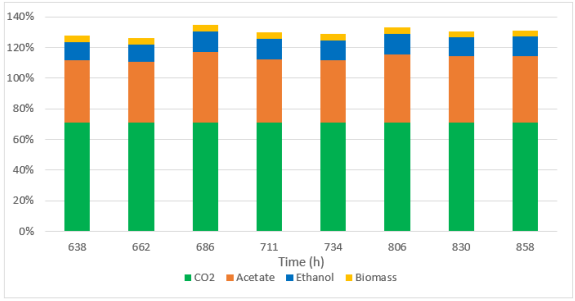

(a) C- balance

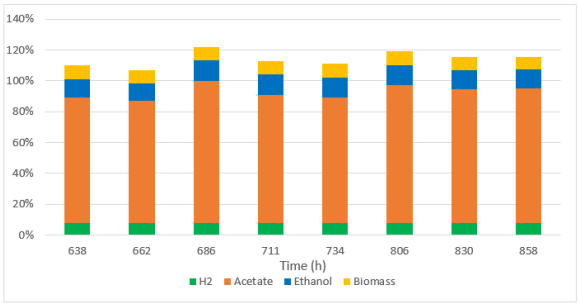

(b) e-balance

Figure B.4: Carbon (a) and electron balance (b) for second steady state after correcting for off-gas values

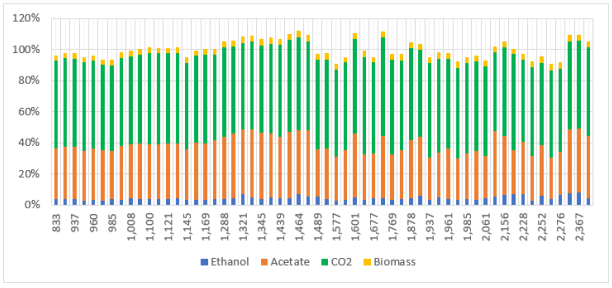

(a) C- balance

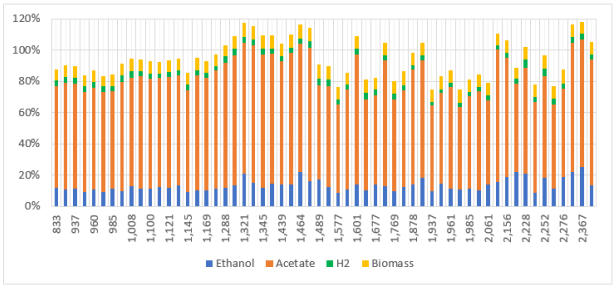

(b) e-balance

Figure B.5: Carbon (a) and electron balance (b) for third steady-state

C Appendix

C.1 Theoretical estimation of kinetic parameters

The maximum biomass specific substrate consumption rate can be estimated using the Herbert-Pirt equation, which defines the relation between the biomass specific substrate consumption rate and the biomass growth and maintenance processes:

$$q_s^{max} = \frac{1}{Y_{X/S}^{max}} * \mu^{max} + m_s \tag{C.1}$$

In order to estimate the maximum substrate uptake rate, the maximum growth rate has first to be determined. Heijnen et al.[32] have proposed that the rate of Gibbs energy generated in catabolism is limited by a maximum catabolic rate of electron transport. Using a Arrhenius correlation, the maximum biomass specific electron-transfer rate in the electron transport chain given in mol e^- $/mol_x/$h is defined as follows:

$$q_e^{cat} = -3 * exp(-\frac{69}{R} * (\frac{1}{T} - \frac{1}{298})) \tag{C.2}$$

where R is the universal gas constant (8.314 kJ/mol/K), and T is the temperature that the fermentation takes place. Next, the maximum catabolic flux can be obtained from the equation below:

$$q_s^{cat} = \frac{q_e^{cat}}{NoEln} = (Y_s^{Met} - Y_s^{An}) * \mu^{max} + Y_s^{Cat} * m \tag{C.3}$$

where NoEln is the number of electrons transferred per mol of electron donor in catabolism which is estimated in Section 2.7 (6.625 e^- for acetate and 6.08 e^- for ethanol), m is the maintenance coefficient and Y_s^{Met}, Y_s^{An} and Y_s^{Cat} are the stoichiometric coefficient of the substrate in metabolism, anabolism and catabolism, which have to be calculated as well.

Since CO is the only carbon and energy source in the system, it serves both as electron donor and acceptor in catabolism and as the carbon source in anabolism. Ammonium, which is found in the mineral medium, serves as the nitrogen source. No separate product reaction takes place since both acetate and ethanol are produced in catabolism but in different catabolic reactions. Finally, biomass is only produced in anabolism and the anabolic reaction is the same for ethanol and acetate because they do not participate in the biomass formation. The chemical formula used for biomass is $CH_{1.8}O_{0.5}N_{0.2}$. The anabolic and catabolic reactions for the two components are given below:

Acetate

$$Anabolism : 2.1CO + 0.2NH_4^+ + 0.6H_2O \rightarrow CH_{1.8}O_{0.5}N_{0.2} + 1.1CO_2 + 0.2H^+ \tag{C.4}$$

$$Catabolism : CO + 0.5H_2O \rightarrow 0.25CH_3COO^- + 0.25H^+ + 0.5CO_2 \tag{C.5}$$

Ethanol

$$Anabolism : 2.1CO + 0.2NH_4^+ + 0.6H_2O \rightarrow CH_{1.8}O_{0.5}N_{0.2} + 1.1CO_2 + 0.2H^+ \tag{C.6}$$

$$Catabolism : CO + 0.5H_2O \rightarrow 0.17C_2H_6O + 0.67CO_2 \tag{C.7}$$

Once the anabolic and catabolic reactions are defined, the microbial metabolism can be determined as follows:

$$Metabolism = \lambda_{cat} * Catabolism + \lambda_{An} Anabolism \tag{C.8}$$

where λ_{cat} is defined as the number of times that catabolism has to run in order to generate sufficient energy to produce one Cmol of biomass. Metabolism is calculated per mole of biomass formed, so λ_{An}

is by definition equal to 1. In order to calculate the λ_{cat}, the Gibbs energy change for the catabolism, anabolism and metabolism have to be determined. First the Gibbs free energy change at chemical standard conditions is calculated:

$$\Delta G^0 = \sum_1^n Gf_{si}^0 * Y_{si} \tag{C.9}$$

where Gf is the standard free energy of formation and Y is the stoichiometric coefficient of the compound in the reaction. Next, the Gibbs free energy is corrected for a pH of 5.5, which is the pH that the fermentation takes place:

$$\Delta G^1 = \Delta G^0 + R * T * ln([1 * 10^{-5.5}]^{Y_{H^+}}) \tag{C.10}$$

Finally, a temperature correction for 37°C is done as follows:

$$\Delta G_R^{1,T} = \Delta G^1 * \frac{T}{T_s} + \Delta H^1 * \frac{T - T_s}{T_s} \tag{C.11}$$

where T is the actual temperature, Ts is the temperature at standard conditions (298.15 K) and ΔH^1 is the standard enthalpy change for the reaction at a pH of 5.5.

Based on these data, the Gibbs energy in catabolism for ethanol and acetate is -33.7 and -37.0 kJ/mol of CO respectively. The Gibbs energy for anabolism is -54.3 kJ/mol of biomass formed.

Heijnen and Van Dijken [31] have suggested a formula which can estimate the energy dissipation per mole of biomass formed for growth when the Gibbs energy change for anabolism is negative. This energy dissipation depends only on the number of the carbon atoms (NoC) and the degree of reduction (γ) of the C-source as shown below:

$$-\Delta G_{Met}^{01} = 200 + 18 * (6 - NoC)^{1.8} + exp[((3.8 - \gamma)^2)^{0.16} * (3.6 + 0.4 * NoC)] \tag{C.12}$$

Carbon monoxide has only 1 carbon atom while its degree of reduction is +2 which results to an energy dissipation of -651.1 kJ/mol of biomass formed. This energy dissipation equals the free energy change of metabolism and it can be correlated with the free energy change of anabolism and catabolism as follows:

$$\Delta G_{Met}^1 = \lambda_{cat} * \Delta G_{Cat}^1 + \Delta G_{An}^1 \tag{C.13}$$

A λ_{cat} of 16.13 and 17.75 is calculated for acetate and ethanol respectively. Going back to Equation C.8, the metabolic reaction can be derived for both acetate and ethanol:

Acetate

$$18.23CO + 0.2NH_4^+ + 8.67H_2O \rightarrow CH_{1.8}O_{0.5}N_{0.2} + 4.033CH_3COO^- + 9.17CO_2 + 4.233H^+ \tag{C.14}$$

Ethanol

$$19.8CO + 0.2NH_4^+ + 9.47H_2O \rightarrow CH_{1.8}O_{0.5}N_{0.2} + 2.96C_2H_6O + 12.9CO_2 + 0.2H^+ \tag{C.15}$$

Since the metabolic reaction was also defined for the two products, the stoichiometric coefficients missing in Equation C.3 are known.

Table C.1: Catabolic, anabolic and metabolic stoichiometric coefficients for ethanol and acetate

Parameters	Ethanol	Acetate
Y_s^{An}	-0.21	-0.21
Y_s^{Cat}	-1.0	-1.0
Y_s^{Met}	-19.8	-18.23

The next step is the derivation of the maintenance coefficient. Maintenance can be derived using the biomass specific Gibbs energy consumption for maintenance, m_G ($kJ/mol_x/h$) as proposed by Tijhuis et al. [33]. A value of 4.5 $kJ/mol_x/h$ was derived by the authors based on data from different microorganisms. The maintenance coefficient can then be estimated as follows:

$$m_s = -\frac{m_G}{\Delta G^{01}_{Cat}} \tag{C.16}$$

A maintenance coefficient of 0.108 and 0.120 $mol_{e^-_{donor}}/mol_X/h$ is found for acetate and ethanol respectively at 298 K (25°C). Equation C.3 finally gives the maximum growth rate at 298 K for the two fermentation products (0.0214 and 0.021 h^{-1} for acetate and ethanol respectively). Correcting these numbers for the temperature of 37°C, the maximum growth rate for ethanol and acetate is 0.064 and 0.063 h^{-1} respectively.

Finally, the only parameter missing to estimate the maximum substrate uptake rate using only the Gibbs free energy of change is the maximum biomass yield which is the substrate yield in metabolism (1.35 g_{DCW}/mol_{CO} and 1.24 g_{DCW}/mol_{CO} for acetate and ethanol respectively). Substituting these values to Equation C.1 results to a maximum substrate consumption rate of 60.0 $mmol_{CO}/g_{DCW}/h$ for acetate and 65.0 $mmol_{CO}/g_{DCW}/h$ for ethanol.

C.2 Estimation of maximum biomass yield using the ATP-balancing method

The biochemical knowledge of the microorganism enabled the estimation of the moles of ATP that are generated in catabolism for acetate and ethanol formation. 1.50 moles of ATP per mole of acetate are produced which it is translated to 0.376 moles of ATP per mole of CO, while 2.05 moles of ATP per mole of ethanol produced gives 0.342 moles of ATP per mole of CO. In that way, the catabolic reaction can be derived including the ATP produced as follows:

Acetate

$$Catabolism: CO + 0.5H_2O \rightarrow 0.25CH_3COO^- + 0.25H^+ + 0.5CO_2 + 0.376ATP \tag{C.17}$$

Ethanol

$$Catabolism: CO + 0.5H_2O \rightarrow 0.17C_2H_6O + 0.67CO_2 + 0.342ATP \tag{C.18}$$

To derive the anabolic reaction, the ATP consumed to produce one C-mole of biomass is needed. Since this number could not be found in literature, the theoretical ATP/X yield for CO_2 (-3.73 moles of ATP/Cmol biomass) was used [34]. This number is valid when the Gibbs energy change for anabolism is negative. Carbon dioxide can serve as the carbon source for *C.autoethanogenum* growth. Therefore, it is assumed that the difference of the ATP requirements between the two carbon sources is not significant. This gives the anabolic reaction considering the ATP investment. The Gibbs energy change for anabolism is -171.2 $kJ/mol_x/h$, which is more than 3 times higher compared to the value calculated using the Gibbs dissipation method (-54.31 $kJ/mol_x/h$).

Acetate

$$Anabolism: 2.1CO + 0.2NH_4^+ + 0.6H_2O + 3.73ATP \rightarrow CH_{1.8}O_{0.5}N_{0.2} + 1.1CO_2 + 0.2H^+ \tag{C.19}$$

Ethanol

$$Anabolism: 2.1CO + 0.2NH_4^+ + 0.6H_2O + 3.73ATP \rightarrow CH_{1.8}O_{0.5}N_{0.2} + 1.1CO_2 + 0.2H^+ \tag{C.20}$$

The ATP produced in catabolism and consumed in anabolism has to be equal. Thus, there is no net production or consumption of ATP, which leads to the following equation:

$$\lambda_{cat} * Y^{Cat}_{ATP} + \lambda_{An} * Y^{An}_{ATP} = 0 \tag{C.21}$$

Since metabolism is defined per 1 Cmol of biomass produced, λ_{An} =1. Using the ATP values for catabolism and anabolism mentioned above, a λ_{cat} of 9.92 and 10.91 is derived for acetate and ethanol respectively. The metabolic reactions are then derived according to Equation C.8. A maximum biomass yield of 2.05 g_{DCW}/mol_{CO} and 1.89 g_{DCW}/mol_{CO} is calculated for acetate and ethanol respectively.

Acetate

$$12.02CO + 0.2NH_4^+ + 5.56H_2O \rightarrow CH_{1.8}O_{0.5}N_{0.2} + 2.48CH_3COO^- + 6.06CO_2 + 2.68H^+ \quad \text{(C.22)}$$

Ethanol

$$13.0CO + 0.2NH_4^+ + 6.053H_2O \rightarrow CH_{1.8}O_{0.5}N_{0.2} + 1.82C_2H_6O + 8.37CO_2 + 0.2H^+ \quad \text{(C.23)}$$

The Gibbs energy dissipated can be finally calculated from the Gibbs energies of formation of the individual components and after correcting for a pH of 5.5 and a temperature of 310 K (37°C). The Gibbs energy change in metabolism for acetate and ethanol equals -421.27 and -421.07 ($kJ/mol_x/h$) respectively. This means that the reaction equations obey the thermodynamic laws, since metabolism is always an exergonic reaction.